Modelling of γ' Precipitation in Superalloys

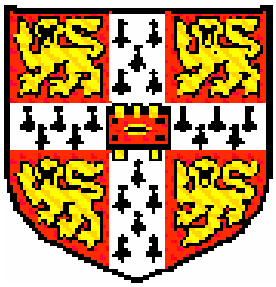

Aikaterini Plati

St. John's College

A dissertation submitted for the
degree of Master of Philosophy
at the University of Cambridge

University of Cambridge

Department of Materials Science and Metallurgy

August 2003

Preface

This dissertation is submitted for the degree of Master of Philosophy in Modelling of Materials at the University of Cambridge. The research described herein was conducted under the supervision of Professor H.K.D.H. Bhadeshia and Dr T. Sourmail in the Department of Materials Science and Metallurgy, University of Cambridge, between May 2003 and August 2003.

This work is to the best of my knowledge original, except where acknowledgements and references are made to previous work. Neither this, nor any substantially similar dissertation has been or is being submitted for any other degree, diploma or other qualification at any other university. This dissertation contains less than 15000 words.

Aikaterini Plati

August 2003

Acknowledgements

I am extremely grateful to my supervisor, Professor H.K.D.H. Bhadeshia for his constant guidance and support, and for his unique way of teaching the simplicity and beauty of everything that surrounds us. I would also like to thank Dr T. Sourmail who helped me begin this project with a smile and significantly contributed to the implementation of the simulation model I used.

I would like to thank all the people in the Phase Transformations and Complex Properties Research Group for all the "happy hours" we shared, and Mathew who was there whenever I needed help with Latex.

I thank all nine chevaliers of the M.Phil. class of 2002/2003 for their friendship and encouragement throughout the year. I would like to thank Helen for the 1001 emails I received from her.

I acknowledge the Engineering and Physical Sciences Research Council for providing me with a scholarship to pursue this M.Phil. degree.

I am extremely grateful to Stavros for his valuable feedback on this thesis and the total confidence he has shown me.

I would also like to thank my family for their love and constant support. I would especially like to thank my grandmother Europi for all the wisdom she gave me throughout this year.

Abstract

Nickel-based superalloys are successfully used as components of aircraft engines and power plants, both marine and land based. They present a high creep resistance and stability at high temperatures. Their mechanical properties depend on the volume fraction, the morphology, and the size distribution of γ' phase. A review is made on previous attempts to model γ' precipitation. All the proposed models failed to predict the nucleation and growth of the fine secondary γ' precipitates in alloys during the ageing stage.

In this project a new physical model is developed that predicts the volume fraction and the average radius of secondary γ' precipitates during alloy ageing. The model uses the basic theory of nucleation and growth, and accesses thermodynamical information from MT-DATA. A binary approximation is made and Al is accepted as the controlling element of the diffusion-controlled growth.

The values of the number of nucleation sites and of the interfacial energy are determined. The model is successfully tested against published experimental data. The sensitivity of the model on different alloy compositions, different ageing temperatures and different cooling rates is analysed.

Contents

List of Figures

Nomenclature and Abbreviations

$\sigma_{a,b}$	the interfacial energy per unit area for an interface between the phases indicated in the subscript
ΔG_v	the Gibbs energy change per unit volume of embryo
ΔG_s	the induced strain energy per unit volume of embryo
G_t^*	the activation energy of nucleation
Q	the Gibbs free energy change per mole of γ' nucleation
r	the radius of the precipitate
r_m	the radious of the precipitate at position m
I	the nucleation rate
R	the gas constant
k	the Boltzmann's constant
h	the Planck constant
T	the absolute temperature of the system
T_{solvus}	the γ' solvus temperature
t	the time
τ	the incubation time
N	the number density of nucleation sites
ρ	the frequency in which an atom attempts to be added to a critical radius
C_i^j	the concentration of element i in phase j
C_i^{jl}	the concentration of element i in phase j in equilibrium with l

$\overline{c_i^j}$	the overage concentration of element i in phase j
v	the interfacial velocity
D_i^j	the volume diffusion coefficient of element i in phase j
J^i	the flux of component i
Ω	the supersaturation
ϕ	the growth rate of the precipitate
x	the precipitate size
V_m	the molar volume of the precipitate
V^j	the volume of phase j
V	the total volume in which the transformation occurs
V_e^j	the extended volume of phase j
V_f^j	the volume fraction of phase j
$V_f e^j$	the extended volume fraction of phase j
β^*	the rate of atomic attachment to the critical nuclei
S	the nucleation scaling factor
Ξ	the order parameter
M_i	the mobility of element i
g	the free energy density
N_i	the atoms per unit volume of phase i
R_c	the cooling rate
MXT	the maximum temperature during a heat treatment
MNT	the minimum temperature during a heat treatment
t_T	the total duration of a heat treatment
D_0	the frequency factor
MT-DATA	Metallurgical and Thermochemical Databank
SGTE	Scientific Group Thermodata Europe
fcc	face-centered cubic
TTT	Time-Temperature-Transformation
CCT	Continuous-Cooling-Transformation

Chapter 1

Introduction

The successful application of some nickel-chromium and iron-based alloys as high temperature components of aircraft, marine, and land-based power systems, led to the designation of "superalloys". In the near future, it will be necessary to increase the steam temperatures in electric generating power plant to 750 °C in order to increase the thermodynamic efficiency. Current steam temperatures are in the vicinity of 600 °C. Nickel alloys containing γ' precipitates (superalloys) have recently been designed specifically for this purpose. The aim of the work presented in this thesis was to model one aspect of the long term microstructural stability, i.e., the γ' precipitates, of these novel alloys.

1.1 Structure of γ' Phase

The main elements that form γ' precipitates are Ni, Al, and Ti. The first full structural determination of γ' phase was made by Betteridge and Franklin in 1957 [7]. Gamma prime or in the present content Ni_3(Al,Ti) is a structural intermetallic compound in superalloys. An intermetallic compound has characteristics of both metals and ceramics with bonding that is a mixture of metallic and covalent bonding [8]. The properties of Ni_3(Al,Ti)

are shown in Table 1.1.

The crystal structure of γ' is $L1_2$(ordered face-centred cubic). The unit cell consists of nickel atoms at the face centres, and Al atoms at the cube corners. Each nickel atom is surrounded by eight other Ni atoms and four Al atoms. Every Al atom has two Ni atoms as its first nearest neighbours, and no other Al atom [7].

Compound	Crystal structure	Melting temp. (°C)	Density (kg m^{-3})
Ni_3(Al,Ti)	$L1_2$ (ordered FCC)	1140	7500

Table 1.1: Physical Properties of $Ni_3(Al, Ti)$ [8]

1.2 Microstructural Evolution and Mechanical Properties

The details of microstructural evolution depend on the heat treatment of the superalloy. Grosdidier [9] performed experiments on different superalloys at 1300 °C with a cooling rate of 150 °C s^{-1} where precipitates were spherical with similar sizes. At a cooling rate of 100 °C s^{-1} γ' precipitates were observed to have a more cubic shape. For the lower cooling rates the precipitates were coarse, erratic, and heterogeneous in size. The shapes of the γ' precipitates transformed from sphere to cube to octocube (by splitting of single precipitates) to octodendrite, and finally to dendrites. The first three types of transformations occur rapidly, whereas the last types are influenced by the impingement of the precipitates so they occur more slowly. Another important observation was that secondary precipitation occurred within the corridors of the γ matrix.

Superalloys in general contain a very high volume fraction of precipitates, often in excess of 0.6.

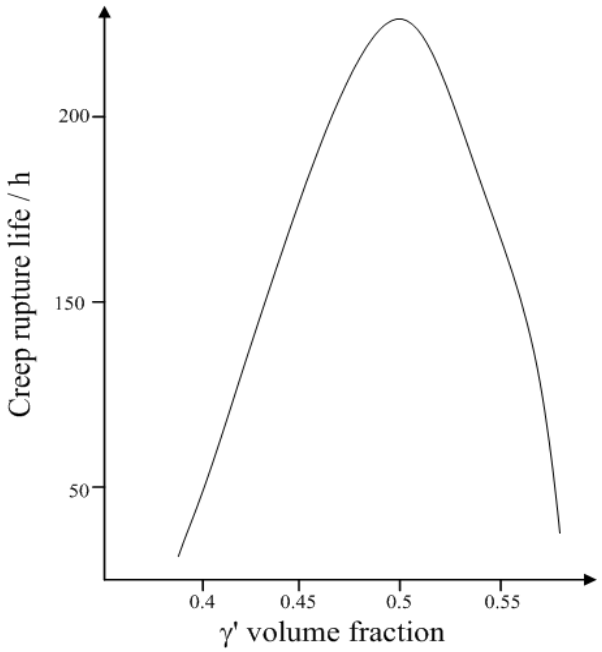

Figure 1.1: Creep rupture life versus γ' volume fraction [1].

The respective amounts some of the main elements that form γ' precipitates, i.e., Al and Ti, control the coherence of the γ' precipitates with the matrix. According to Baldan [1] observations on an IN-100 superalloy, the creep rupture life of the superalloy strongly depends on the γ' volume fraction. When the γ' volume fraction of secondary precipitates is increased up to 0.5 the creep rupture life increases. At volume fractions that exceed 0.5 there is a sudden decrease of the creep rupture life, as illustrated in Figure 1.1.

The composition of some typical commercial superalloys is shown in Table 1.2. Cobalt improves the temperature stability of the γ' phase. Chromium and aluminum are elements which protect from oxidation and corrosion, by forming thin oxides layers adherent to the surface [10]. Carbon, niobium, tantalum, molybdenum, titanium, and chromium lead to carbide precipitation in superalloys. Boron and zirconium inhibit the formation of the carbides and reduce the solubility of carbon at the grain boundaries. Carbides of

small size are beneficial since they reduce the grain boundary sliding and, therefore, delay the onset of creep rupture [11].

Elements such as Pb, Bi, Sb, As, S, P, and Ag are detrimental as they form a low melting point film on the grain boundaries and lower the creep resistance [10].

Composition (wt%)	Ni	Cr	Co	Ti	Al	Mo	C	B	Fe	Si
Astroloy	balance	15.0	17.0	3.5	4.0	5.25	0.06	0.030	-	-
Inco1	balance	7.1	19.0	3.0	0.9	0.6	3.0	0.04	20	(Nb 5.2)
Inconel	42.0	9.1	13.0	-	3.0	0.3	5.7	0.04	-	balance
IN-100	balance	10.0	15.0	4.7	5.5	3.0	0.18	0.014	(Zr 0.06)	(V 0.1)

Table 1.2: Composition of Different Superalloys [12]

1.3 Problem Statement

There is a need to understand both qualitatively and quantitatively the precipitation of γ' in order to characterise the microstructure of a superalloy.

The main objective of this research is to develop a model that will give a quantitative estimation of the volume fraction of secondary γ' precipitates as a function of composition and heat treatment. This is accomplished here through a physical model that uses the basic theories of nucleation and growth, and accepts Al as the element that controls the diffusion-controlled growth. This model interfaces with MT-DATA to access thermodynamic information, thereby limiting the empirical input parameters. It also calculates the growth of the average radius of γ' by imposing a simple sphere shape on the particle.

The accuracy of the results is tested against published experimental data. Validating the results of the model provides further information that may aid in understanding the transformation mechanism of γ' precipitation, and its dependence on composition, temperature, and cooling rates during ageing.

1.4 Thesis Organisation

This thesis is organised in 5 chapters as follows.

Chapter 2 presents the basic theories of nucleation and growth, and examines a number of different approaches that have been adopted for determining γ' precipitation. In particular the Zener model and the Avrami theory are presented and the McLean, Gabb *et al.*, and Carter *et al.* models are examined.

Chapter 3 introduces a new computational model that predicts the secondary γ' volume fraction during different heat treatments. It begins with a brief discussion of MT-DATA, a software package dealing with thermodynamics. Next it presents the nucleation and growth theory that the model is based on, and it then justifies the choice of Al as the controlling element for the diffusion-controlled growth of γ' precipitates. The chapter concludes with a description of the implementation of the model.

Chapter 4 presents the stimulation results. The input parameters of the simulation model, number of nucleation sites and interfacial energy, are first estimated using part of the experimental data, and then compared to published empirical results. The sensitivity of the model is analysed by varying the superalloys composition, the ageing temperatures and cooling rates.

Chapter 5 presents an overall evaluation of the model, and proposes ways of improving the model so that it can predict the γ' volume fraction more accurately .

Chapter 2

Theory and Modelling of Overall Transformation Kinetics

It is useful to model the growth and understand the kinetics of γ' precipitation in order to be able to determine the growth rate of γ' and its dependence on time and supersaturation. In this chapter we examine a number of approaches that have been adopted for determining the growth rate of γ' precipitation.

2.1 Theory of Nucleation

According to the classical nucleation theory [8], the activation Gibbs energy G^* for a spherical nucleus is:

$$G^* = \frac{16\pi}{3} \frac{\sigma_{a,b}^3}{(\Delta G_v + \Delta G_s)^2} \tag{2.1}$$

where $\sigma_{a,b}$ is the interfacial energy per unit area between two phases a, b, ΔG_v is the magnitude of the Gibbs energy change per unit volume of embryo, and

ΔG_s is the induced strain energy per unit volume of embryo.

If we assume that ΔG_v and ΔG_s are not dependent on the radius of the nuclei, then the critical radius of a nuclei r_c is given by:

$$r_c = -\frac{2\sigma_{a,b}}{\Delta G_v + \Delta G_s} \tag{2.2}$$

The nucleation rate I is:

$$I = N \exp(-\frac{G^*}{RT})\rho \exp(-\frac{G_t^*}{RT}) \tag{2.3}$$

where ρ is the frequency at which an atom attempts to be added to a critical radius, N is the number density of nucleation sites, R is the gas constant, T is the absolute temperature, and G_t^* is the activation energy of transfer across the interface [8].

2.1.1 Heterogeneous Nucleation

Nucleation in solids is almost always heterogeneous. Sites which are suitable for nucleation are non-equilibrium defects, such as dislocations and grain boundaries. In these cases the creation of a nucleus results in the destruction of a defect and, hence, a reduction of the activation energy barrier. The equations for the nucleation rate are a function of a shape factor and of the dislocation density.

Due to the strong dependency of the nucleation rate on N and σ, the homogeneous rate equation is best conceived as a fitting equation. Therefore, there is little to gain in practice by using more complex models.

2.2 Theory of Growth and Coarsening

There are three different rate-controlling processes of growth: diffusion-controlled growth, interface-controlled growth, and mixed-controlled growth.

Diffusion-controlled growth occurs when diffusion through the bulk to the interface is the rate-limiting process. The interface composition, therefore, is assumed to be the equilibrium one. When it is difficult for the atoms to jump across the interface, the interface composition can deviate from equilibrium and growth is said to be interface-controlled. Mixed-controlled growth as the name implies is a combination of the two previous rate-controlling processes.

It is generally assumed that most precipitation phenomena occur at relatively high-temperature are diffusion-controlled.

According to Fick's second Law:

$$\frac{\partial C^i}{\partial t} = -\mathrm{div} J \tag{2.4}$$

where i can be either the matrix (b) or the precipitate (a), C^i is the concentration of solute in phase i, and J^i is the diffusion flux. If we consider one way diffusion at the interface ϕ of the precipitate the following equation must be satisfied:

$$\phi(C^{ab} - C^{ba}) = |J_{r=r_m}| \tag{2.5}$$

where C^{ab} is the concentration of solute in the precipitate a in equilibrium with the matrix b, and C^{ba} is the composition of the concentration of the solute in the matrix in equilibrium with the precipitate, and r_m is the position of the interface.

2.2.1 Zener Model

Zener [8] proposed a simple solution to this problem whereby the precipitate has a constant concentration C^a and the gradient ahead of the interface is constant. According to Figure 2.1 the conservation of the mass of the solute implies that:

$$\frac{(C^{ba} - C^m)dx}{2} = x(C^m - C^{ab}) \tag{2.6}$$

where C^m is the concentration of the bulk, dx is the diffusion distance and x is the precipitate size. It is often the case that C^m is almost equal to C^a, therefore it is safe to assume that $(C^{ba} - C^m)$ is almost equal to $(C^{ba} - C^{ab})$, combining the above equations and setting $\Omega = (C^m - C^{ab})/(C^{ba} - C^{ab})$, the following is obtained:

$$x \simeq \Omega\sqrt{Dt} \tag{2.7}$$

where Ω is the supersaturation and takes values from 0 to 1. This proves that the thickening of the particle is related to the square root of time also known as the parabolic growth law [13].

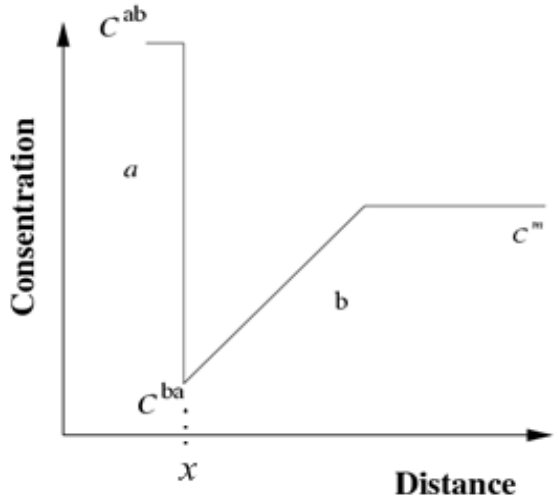

Figure 2.1: Concentration profile at the interface during diffusion-controlled growth (Zener model).

The first derivative of the former equation gives the velocity of the interface [8]:

$$\frac{dx}{dt} \simeq \frac{\Omega\sqrt{D}}{2\sqrt{t}} \tag{2.8}$$

For small supersaturations ($\Omega \longrightarrow 0$) the diffusion is kinetically not favoured, while for large supersaturations ($\Omega \longrightarrow 1$) the precipitation process happens instantly.

2.2.2 Spherical Particles

The parabolic growth law can be extended to a two-dimensional and a three-dimensional growth. The exact interface compositions are modified by the shape of the particles according to capillarity theory, whereby the equilibrium is affected by the curvature of the interface between precipitate and matrix.

For a spherical particle of radius, r, the interface composition deviates from equilibrium according to [4]:

$$C^{ab} = C^e \exp(\frac{2\sigma_{ab}V_m^b}{RTr}) \tag{2.9}$$

where C^e is the equilibrium solute in the matrix and V_m^b is the molar volume of the b precipitate.

For multicomponent systems, this is described by and is given by [14]:

$$(\Delta C^{ab}][G][\Delta C^b) = \frac{2\sigma_{ab}V_m^b}{r} \tag{2.10}$$

where (] indicates a row vector, [) a column vector, and $[G]$ is the hessian of the Gibbs energy as a function of composition.

2.3 Overall Kinetics

This section deals with methods available for modelling the overall kinetics of transformation occurring by nucleation and growth.

2.3.1 Avrami Theory

Avrami [8] proposed a theory based on nucleation and isothermal growth, assuming that nucleation occurs at certain sites which are gradually exhausted. Using the concept of extended volume, V_e^a (the sum of the volumes of all the precipitate particles), Avrami, Mehl, Johnson, and Kolmogorov

expressed the change in the volume of phase a as follows:

$$dV^a = (1 - \frac{V^a}{V})V_e^j \tag{2.11}$$

where V^a is the volume of phase a and V is the total volume.

For a random distribution of precipitate particles integrating the former equation results in the volume fraction V_f^a of phase a as follows:

$$V_f^a = 1 - \exp(-\frac{V_e^a}{V}) \tag{2.12}$$

The extended volume V_e^a is calculated using nucleation and growth models and neglecting any impigement effects. This results in the volume fraction V_f^a of phase a as follows:

$$V_f^a = 1 - \exp(-z_a t^n) \tag{2.13}$$

where n is a numerical exponent that can take values from 1 to 4. If we assume a one-dimensional growth then $1 < n < 2$, in the case of a two-dimensional growth $2 < n < 3$, and $3 < n < 4$ for a three-dimensional growth. z_a depends on the nucleation and growth rates and its values are sensitive to temperature [10]. The correction made for the extended volume leads to a loss of information, therefore, the precipitate size distribution of this model is not cannot be predicted.

2.3.2 Growth in Ternary Systems

Growth in ternary systems is treated either by using a binary approximation (accepting that the growth rate is determined by the diffusivity of one component), or by using the tie-line method.

In the case of a multicomponent system where one component diffuses at least an order of magnitude faster than the other one ($D_1 \ll D_2$), the binary approximation is not reasonable because it does not ensure mass balance for all the elements involved in the transformation. For the case where $D_1 \ll D_2$,

Coates (1973) [15], [16] introduced a model for diffusion-controlled precipitate growth in ternary systems where he used a flux-balanced tie-line. In the case of high supersaturation, according to his model, he chose a tie-line that greatly increase the gradient of the component with the lower diffusion coefficient, to compensate for its low diffusivity. In the case of low supersaturation a tie-line that reduces the gradient of the component with the higher diffusion coefficient is chosen, this is depicted in Figure 2.2. The appropriate tie-line was identified by drawing a vertical line through the point P, corresponding to the bulk composition of the alloy. As a result of Coates assumptions, the gradient of component 2, increase to compensate for its low diffusivity, as illustrated in Figure 2.2.

Fujita and Bhadeshia (1999) [17] approximated the flux-balanced tie-line by reducing the gradient of the fastest element to zero. Following Coates, they introduced tie-line shifting that could deal with changes in the matrix composition.

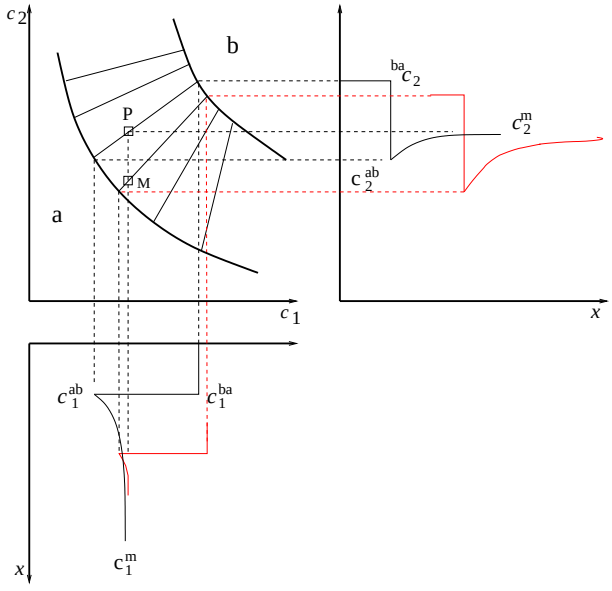

Figure 2.2: Flux tie-line based on Coates model [2].

Sourmail [2] modified and extended Coates model, to systems with more

than three components. Instead of using an isoconcentration tie-line he used an isoactivity tie-line. This implies that the activity of the fastest diffusing element is assumed to be equal to the far field one. Again, the velocity of the interface is assumed to be given by the diffusion of the slow component using the new calculated tie-line. This leads to a prediction of the precipitate growth and provides a better fit with the experimental results as shown in Figure 2.3.

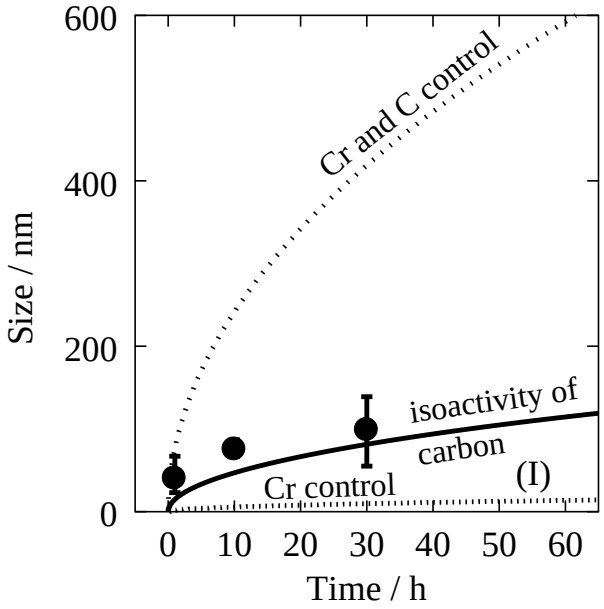

Figure 2.3: Radius of $M_{23}C_6$ at 650 °C [2].

2.4 Models of γ' Precipitation

This section examines different models that have been developed for the precipitation of γ' precipitates in superalloys. Specifically, the McLean, Gabb *et al.*, and Carter *et al.* models are considered.

2.4.1 McLean Model

McLean (1984) [3] attempted to predict the growth of γ' precipitates in nickel alloys using two different laws. The first law was supposed to describe diffusion-controlled growth. The second law was supposed to describe an interface-controlled reaction. The first and the second laws are expressed as:

$$r = (kt)^{\frac{1}{3}} \tag{2.14}$$

$$r = (k^{'}t)^{\frac{1}{2}} \tag{2.15}$$

where k is a constant and has the form:

$$k = \frac{ADC\sigma V_m}{RT} \tag{2.16}$$

where A is a constant of proportionality, C is the Al content of the matrix, D is the Al diffusion coefficient, σ is the interfacial energy, V_m is the molar volume of the γ' precipitate. In McLean's model C, was provided from experimental results obtained in the literature, and σ was an estimated fitted parameter that produced results that matched the experimental data. Figure 2.4 illustrate the experimental data plotted according to the first and the second law. The fit to the results is excellent, according to Figure 2.4, nevertheless, the Model that McLean used is based on a fitted parameter, (σ), and on experimental data, (C). Furthermore, the first law that McLean used does not describe diffusion-controlled growth but coarsening, hence, it has a nice fit over a large range of time. The second law does not correspond to interface-controlled growth but to diffusion-controlled growth, thus, it is not valid for a long ageing time were precipitate coarsening is the dominating process. Furhtermore McLean's model does not consider nucleation events.

Irisarri *et al.* (1985) [18] used the same theory and proposed a kinetic law for the mixed-controlled growth according to which $f(r_m/2) = (8/9)(r_m/3)^3 + (D/\sigma)(r_m/2)^2$. Effectively this is the sum of the two pre-

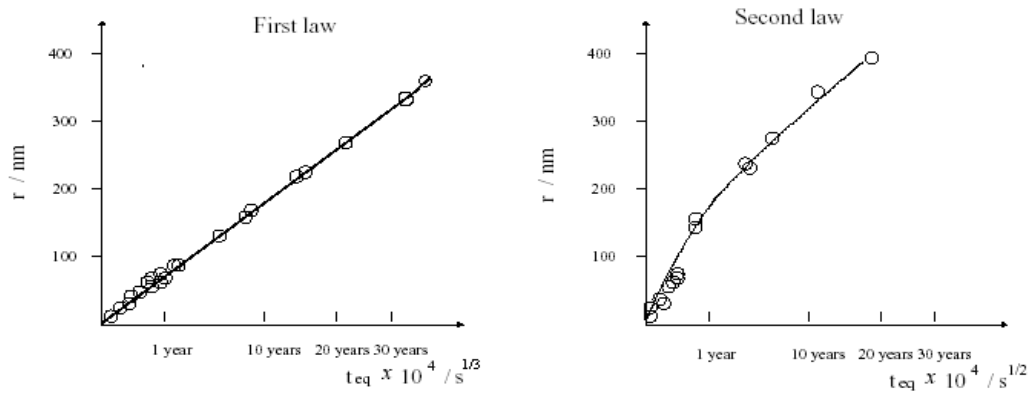

Figure 2.4: First and Second law (McLean model) fitted on experimental data (time, t, under a given combination of ageing temperature, T, and Al content of the matrix, C, is recalculated as equivalent time (t_{eq}), thus bringing all the growth data to a common time base) [3].

vious laws. Based on experimental data Irisarri *et al.* suggested that the mixed-controlled growth process controls γ' precipitate growth.

2.4.2 Gabb *et al.* Model

Gabb *et al.* [4] introduced a simple kinetic model to predict the nucleation and growth of γ' precipitates in oil quenched disks (manufactured for aircraft turbines). The model is based on the basic nucleation and growth theories which have been introduced earlier (Section 2.1 and Section 2.2) using a binary approximation, and predicts the γ' precipitate coarsening and size distribution as a function of the thermal history of the alloy. The model elements are as follows:

- The ternary Ni-Al-Ti system is treated as a binary Ni-(Al+Ti). The γ' volume fraction $V_{f\gamma'}$ is expressed as:

$$V_{f\gamma'} = \frac{C_o(1 - \exp(-\frac{Q}{R}(\frac{1}{T} - \frac{1}{T_{solvus}})))}{C_{\gamma'} - C_o \exp(-\frac{Q}{R}(\frac{1}{T} - \frac{1}{T_{solvus}}))} \tag{2.17}$$

  where $C_{\gamma'}$ is the Al+Ti composition in γ', C_o is the initial Al+Ti composition in the alloy, Q is the Gibbs free energy change per mole of γ'

nucleation, and T_{solvus} is the γ' solvus temperature. A number of tests were used to correlate the constant, Q, as a function of temperature, since the precipitate composition is considered independently from the temperature.

- A kinetic model is used to express the onset of nucleation and classical nucleation theory is used to express the nucleation of a spherical nuclei. According to their model the isothermal nucleation rate I is given by:

$$I = N[G^*/(3\pi kT)]^{1/2}\beta^*\exp(-G^*/kT)\exp(-\tau/t) \tag{2.18}$$

where N is the density of active nucleation sites per unit volume, G^* is the activation Gibbs energy for nucleation, τ is the incubation time to form embryos before nucleation, and β^* is the rate of atomic attachment to the critical nuclei. Assuming growth controlled by the slowest diffusion species, the diffusion coefficient D is derived from the calibration of the model. The nucleation scaling factor, S, and the interfacial energy, σ, are fitting parameters.

- The growth stage is dealt with using the methods introduced in Section 2.2.1 for diffusion-controlled growth (in the case of a binary system). The diffusion coefficient, D, is a parameter fitted to the experimental results.

- The final element deals with the particle coarsening (change of the precipitate size due to the fact that small particles tend to dissolve, while larger grow). The general form of precipitation coarsening is given by the following equation:

$$\frac{dr}{dt} = \frac{2DC_e\sigma V_m}{RTr(C^{\gamma'} - C_e)}(\frac{1}{r_m} - \frac{1}{r})(1 + br) \tag{2.19}$$

where b is a correction factor for large volume fraction effects. This correction factor is neglected during calculations in order to retain size distribution information.

All the elements are integrated into a computer model as shown in the flow diagram, as illustrated in Figure 2.5.

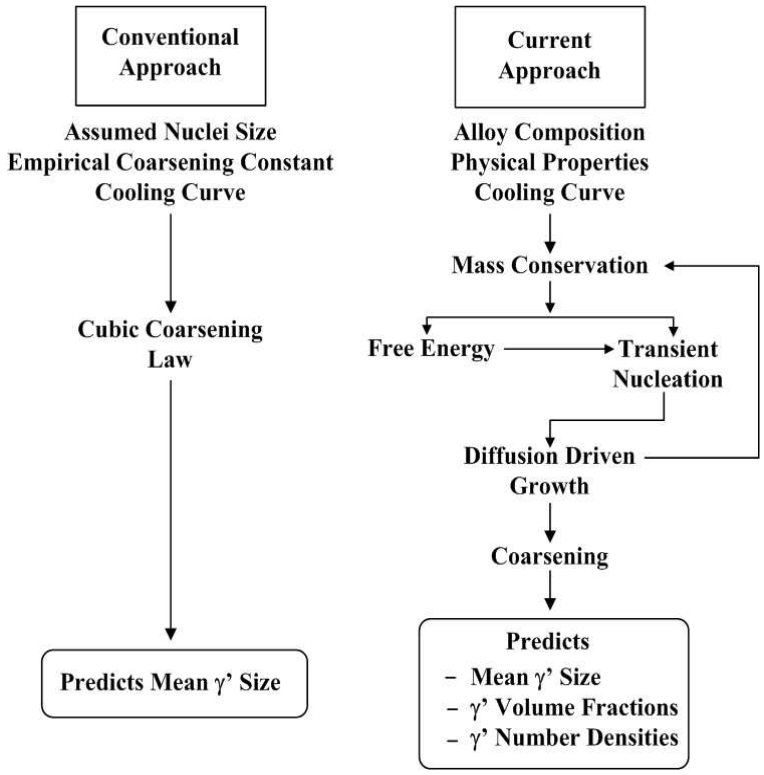

Figure 2.5: Gabbs *et al.* method flow-chart [4].

This model gives a reasonable prediction of the γ' size, and γ' volume fraction. This is illustrated in Figure 2.6. However, Gabbs *et al.* model cannot deal with large volume fractions since it does not take into account the correction, b, for the modelling of the coarsening process . The model uses four fitting parameters making it difficult to use due to its dependence on experiments. Moreover, this model can only deal with quenching and not with multiple step heat treatments.

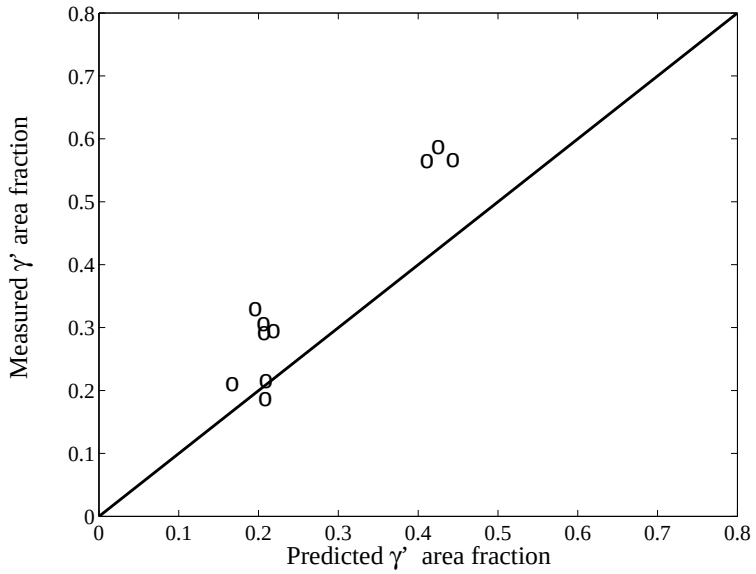

Figure 2.6: Comparison of measured and predicted γ' volume fraction based on Gabb *et al.* model[4].

2.4.3 Carter *et al.* Model

Carter *et al.* examined the growth of γ' precipitates in the Ni-Al-Ti ternary alloy, in the temperature range from 900 °C to 1200 °C. A process involving diffusion-controlled in one dimension with local equilibrium at the γ/γ' interface is accepted.

Fick's second law for a ternary system is given by:

$$\frac{\partial C_{\mathrm{Al}}}{\partial t} = \frac{\partial (D^{\mathrm{Ni}}_{\mathrm{AlAl}} \frac{\partial C_{\mathrm{Al}}}{\partial x})}{\partial x} + \frac{\partial (D^{\mathrm{Ni}}_{\mathrm{AlTi}} \frac{\partial C_{\mathrm{Ti}}}{\partial x})}{\partial x} \tag{2.20}$$

$D^{\mathrm{Ni}}_{\mathrm{AlAl}}$ is the direct diffusion coefficient of Al to the NiAl matrix and $D^{\mathrm{Ni}}_{\mathrm{AlTi}}$ is the indirect diffusion coefficient of Al on the NiTi matrix. Equations of the same form can be used for Ti. To estimate the direct coefficient, a method developed by Whittle and Green for binary systems is used [7]. This method also extends to ternary systems.

Equation 2.7 as described in Section 2.2.4, can also be written as:

$$r = St^{\frac{1}{2}} \tag{2.21}$$

where S is a parabolic rate constant given as a function of the supersaturation, Ω, and Al diffusion coefficient. The model results are shown to agree with the experimental results, proving that the γ/γ' interface moves parabolically with time. It can also been shown that increasing the Ti:Al ratio reduces the growing rate, S, of the γ' precipitate. Thermo-Calc software was used to identify the $\gamma/\gamma+\gamma'$and the $\gamma'/\gamma+\gamma'$ phase boundaries and confirmed the experimental results. According to the calculations, Ti changes the parabolic rate, S, via changes in the interface compositions rather than via changes to the interdiffusion coefficients. As result, this alters the supersaturations.

The direct diffusion coefficients $D^{\mathrm{Ni}}_{\mathrm{AlAl}}$ and $D^{\mathrm{Ni}}_{\mathrm{TiTi}}$ were found to be almost equal or larger compared to the indirect diffusion coefficients for the same temperature. Their values varied from 34×10^{-16} $\mathrm{m^2 s^{-1}}$ to 839×10^{-16} $\mathrm{m^2 s^{-1}}$ respectively.

2.5 Phase Field Modelling

The phase field [5] method is a microstructural evolution simulation method. It is a fairly recent and simple method that produces realistic microstructures. The entire microstructure is represented by one or more order parameters labeled as Ξ. If Ξ takes the value 1 for the precipitate and the value 0 for the matrix, then the values of $0< \Xi < 1$ represent the interface (Figure 2.7).

The evolution of the microstructure with time (the rate of change of the order parameter Ξ) is given by the following equation:

$$\frac{\partial \Xi}{\partial t} = M \frac{\partial g}{\partial \Xi} \tag{2.22}$$

where M is the mobility and g is the free energy density. The free energy density is given in terms of Ξ and its gradient:

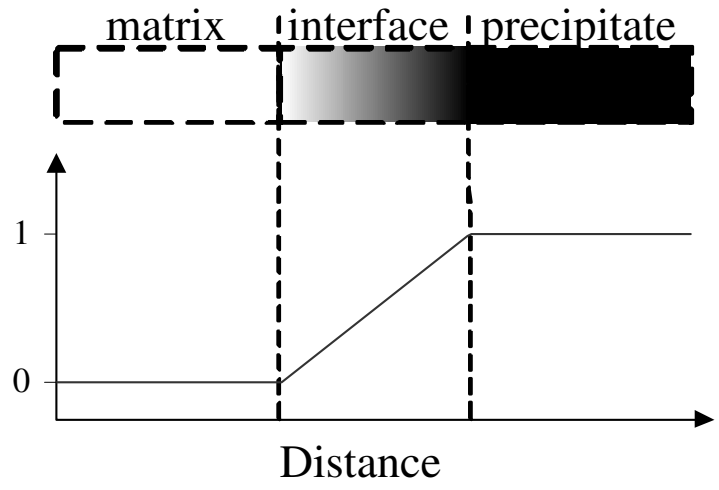

Figure 2.7: Phase field model where the order parameter Ξ takes the value 0 representing the matrix, and the value 1 representing the precipitate [5].

$$g = \int_V [g_o(\Xi, T) + \frac{\epsilon^2}{2}|\nabla\Xi|^2]dV \tag{2.23}$$

where V is the volume and $g_o(\Xi, T)$ is the homogeneous free energy, the sum of the free energy of the precipitate and the matrix.

One of the advantages of the phase field method is that it can treat systems with high volume fractions, i.e., more than 0.50, and can account for elastic interactions between the precipitates and the matrix.

2.5.1 Simmons *et al.* Model

Simmons *et al.* [19] made some improvements to the phase field method and adapted it to conditions of concurrent nucleation and growth in order to model γ' precipitation in superalloys. Their approach has two algorithms which alternate, one for nucleation, and one for growth and coarsening.

The nucleation phase is treated in the first algorithm. The sample is grided into individual cells according to the phase field method, using the classical theory of nucleation. According to their method, both time and

length dimensions need to be scaled up so that they can comply with two basic assumptions that they make for the nucleation phase. They assumed that only one nucleus can be formed in one cell and that the growth rate of a newly formed nucleus is sufficient to inhibit the nucleation of a second precipitate. The growth and coarsening is modelled by using the 2-D phase field method as described in phase field modelling.

Simmons *et al.* method has the ability to successfully predict the microstructure of a binary system taking into account the nucleation. Nevertheless, it can only treat homogeneous nucleation and it cannot be used for cooling processes in alloy systems.

2.6 Summary

A review of the literature indicates that little work has been done on the modelling of the growth of γ' precipitates in Ni-based superalloys. Previous attempts on modelling have been investigated in this chapter. Zener's model is the simplest analytical approach to the diffusion-controlled growth and it is applied in binary systems. McLean attempted to predict γ' precipitation based on a parabolic and a cubic root growth rate law. Coates, introduced a

model using a flux-balance tie-line for diffusion-controlled growth in ternary systems. Improvements to the former mentioned model were made by Bhadeshia and Fujita. This led Sourmail to choose an isoactivity tie-line providing a better approximation for the ternary system. Simmons *et al.* adapted the phase field method and did some improvements which led to a refined prediction not only of the growth rate of γ' precipitates but also of the microstructure evolution of a superalloy.

Based on these observations, it is useful to develop a new analytical method that will be applied to γ-γ' phase transformation and predict the γ' precipitation growth of multicomponent and multiphase systems.

Chapter 3

Simulation Model and Methodology for γ' Precipitation

In Chapter 2, the different models for nucleation and growth that have been traditionally used, were examined. In this chapter, a new computational model for predicting γ' precipitation is introduced, beginning with a discussion of MT-DATA, a software package dealing with thermodynamics. This is followed by an analysis of the different components of the overall transformation kinetics that are used by the model. The chapter concludes with a description of the model implementation.

3.1 MT-DATA

MT-DATA [20] is a software package created in 1970 at the National Physical Laboratory that enables the prediction of the phase behavior of complex, multicomponent systems based on the extrapolation of thermodynamic properties.

MT-DATA is based on a system of equations that can calculate the Gibbs

energy and the heat capacity of a given alloy. Essentially, it minimises the Gibbs energy of a system, thereby finding the equilibrium volume fraction and the composition of the phases that are present [20].

The Gibbs energy of a system can be written as a function of the phases present in the system:

$$G_s = N_\gamma G_\gamma + N_{\gamma'} G_{\gamma'} + ... \tag{3.1}$$

where G_s is the molar Gibbs energy of the system and G_γ and $G_{\gamma'}$ are the molar Gibbs energies of the γ and γ' phases respectively. N_γ and $N_{\gamma'}$ is the number of moles of each phase [20].

The Gibbs energy of each phase is a function of its composition, temperature, and pressure. Consequently, the parameters that are needed to calculate the Gibbs energy of each phase can be physically controlled in practice.

A range of fundamental thermodynamic data that cover a wide variety of systems is readily available with MT-DATA. As long as the user specifies the elements present in the alloy, the initial composition, the temperature, the pressure, and the appropriate source of data, MT-DATA can perform a variety of calculations [21].

The databases used by MT-DATA are under continuous development. In situations where data are missing, MT-DATA displays error messages accordingly.

There are also a number of elements for which MT-DATA has insufficient parameters at present and, therefore, cannot be included in the equilibrium calculations of the system, e.g., V, Si, Mn, P, S, and Ce. These elements are less than 1 wt%, and are not assumed to interfere with gamma prime precipitation.

Overall, MT-DATA is a useful thermodynamical tool for predicting phases that exist in a system but the reliability of the predictions will depend on the amount of data available for the different sub-systems. MT-DATA can-

not predict the evolution of the microstructure. A suitable model that will interact with MT-DATA is required to predict the volume fraction of gamma prime precipitation as a function of time.

3.2 Solution Treatment

During the first stage of a typical superalloy heat-treatment, primary γ' particles are formed rapidly in the matrix at a high temperature. The precipitates at this state are formed by a mechanism that involves the diffusion of substitutional atoms.

The starting equilibrium microstructure is expected to contain small amounts of γ' precipitates. According to experimental data for primary γ' precipitates, the number of density of these particles is shown to be small [22]. The model developed here takes into account the change of the matrix concentration caused by the solution treatment. It interfaces with MT-DATA to obtain the equilibrium composition of the matrix at the temperature of the solution treatment. The growth of the primary γ' precipitates is not calculated since the number density of the primary precipitates is small [23]. The model calculates the volume fraction of the secondary γ' particles that are formed during cooling and modified by subsequent ageing.

3.3 Nucleation

Classical theory of nucleation, presented in Section 2.1, Chapter 2, is used to estimate the nucleation rate for γ' phase [8]:

$$I = N\frac{kT}{h}\exp\{-\frac{G^* + G_t^*}{kT}\} \tag{3.2}$$

where G^* is the activation energy for the nucleation of γ' and G_t^* is the activation energy for transfer of atoms across the γ-γ' interface. N is the

number density of nucleation sites, h and k are the Planck and Boltzmann constants.

ΔG is the energy change that corresponds to the Gibbs energy required for the reaction : $\gamma \longrightarrow \gamma' + \gamma$. ΔG is given by the following equation:

$$\Delta G = N_{\gamma'} G_{\gamma'} - N_{\gamma} G\gamma \tag{3.3}$$

where N_{gamma} is the number of moles of components in γ phase, $N_{\gamma'}$ is the number of moles of components in γ' phase, G_{γ} and $G_{\gamma'}$ are the Gibbs energies per mole of component of the γ and γ' phases respectively [2].

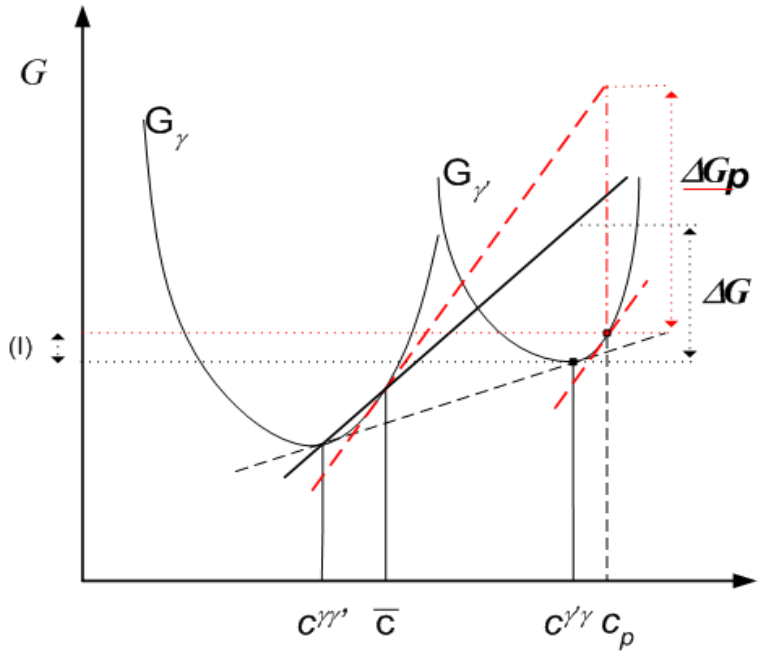

Figure 3.1: The parallel tangent construction for γ' precipitates. The driving force of nucleation as illustrated here is ΔG_p. The most probable composition for the nucleus of γ' (the composition for which the driving force of nucleation is maximum), C_p, is different from the equilibrium composition, $C^{\gamma'\gamma}$. The Gibbs energy of the most probable composition is different from that of the equilibrium composition (I) [2].

There is a need to include the contribution of the composition change in equation 3.4 to estimate correctly the driving force for nucleation. Figure 3.1 illustrates the method of parallel tangent construction that includes the

contribution of composition changes and gives a more correct value of the driving force for nucleation, ΔG_p. As the number of components increases, the method of parallel tangents becomes more difficult to solve. Furthermore, the Gibbs energy of all the phases involved, as a function of composition, is not easily accessible.

To avoid all the previous mentioned difficulties, the program developed here accesses information from MT-DATA to calculate the driving force for γ' precipitate nucleation at each stage of the process. In every iteration the composition change of the system is included so that MT-DATA can perform thermodynamic calculations with the use of Scientific Group Thermodata Europe (SGTE) databases [20]. MT-DATA calculates the simultaneous formation of phases other than γ', therefore, it allows interactions with the composition changes (as supersaturation is reduced) to be properly taken into account as a function of time.

3.4 Growth

To obtain the growth rate of γ' phase the classical Zener model is applied. According to the Zener model the γ' precipitates have a constant concentration and the gradient ahead of the interface is constant in the case of spherical precipitates.

In the Zener model, the radius of the precipitate is related to the square root of time. During a time step, the program calculates the radius increase of γ' precipitates and the volume of the γ' phase.

The extended volume is used in order to take into account hard impingements, the program calculates the extended volume fraction of γ' phase,$V_{fe}^{\gamma'}$, as follows:

$$V_{fe}^{\gamma'} = \sum_{i=0}^{i=k} Nu_i(\frac{4\pi}{3}r_i^3) \tag{3.4}$$

where k is the number of time steps used in the program, and Nu_i is the

number of γ' precipitates nucleated at time step i and which have (growth is considered) a radius r_i. During a time step the program considers all the different phases that excist in the alloy. According to Avrami theory, the volume increase of γ' phase has to be corrected as follows:

$$dV_f^{\gamma'} = (1 - \sum_k V_f^k) dV_{fe}^{\gamma'} \tag{3.5}$$

where $dV_f^{\gamma'}$ is the change in the volume fraction of the γ' phase and $dV_{fe}^{\gamma'}$ is the change in the extended volume fraction of the γ' phase. V_f^k is the volume fraction of a phase k. This correction needs to be applied to each time step since the volume fraction of γ' precipitates in superalloys is relatively high up to even 0.69 [24]. The matrix composition changes are calculated as follows:

$$d\overline{C_i} = \frac{(\overline{C_i} - C_i^{\gamma'\gamma}) dV_f^{\gamma'} - \overline{C_i}}{(1 - \sum_k V_f^k)} \tag{3.6}$$

where $d\overline{C_i}$ is the change of matrix composition of component i, $\overline{C_i}$ is the existing matrix composition, $C_i^{\gamma'\gamma}$ is the composition of component i in the γ' phase which is in equilibrium with γ phase. At the end of each time step the program calculates the composition changes due to γ' precipitate nucleation and growth, and the matrix composition is updated. The time step must be kept small enough so that the composition change will be small compared to the content of the matrix. Small time steps should be used especially when the heat treatment involves quenching of the alloy. A proper time step will prevent a dramatic change of the matrix composition due to a sudden temperature change.

3.5 Temperature Changes

The program analysing the nucleation and growth of γ' precipitates at constant temperature, can also emulate different cooling rates and quenching.

As input, the program requests the number of different temperature treatments, the higher and lower temperature during each treatment, and the duration of each treatment. Taking the given inputs, and applying them to the following equations, the program calculates the cooling rate R_c and the temperature, T, at each time step:

$$T = MXT - t_c R_c \tag{3.7}$$

$$R_c = \frac{MXT - MNT}{t_T} \tag{3.8}$$

where MXT and MNT is the maximum and minimum temperature applied at each heat treatment, t_c is the current time that the temperature is being calculated and t_T is the total duration of each heat treatment. Temperature is a very important parameter in the program, since it has a significant influence on the nucleation and growth of the precipitate. MT-DATA requires temperature as an input at each time step for the calculation of γ' nucleation and the equilibrium concentration. Furthermore temperature changes have a strong influence on the diffusion coefficient which in turn influences the growth rate of the precipitates.

3.6 Diffusion Coefficient

For diffusion-controlled growth, in a multicomponent alloy and assuming local equilibrium at the $\gamma\gamma$' interface, the interface mass conservation condition for all the precipitate components satisfy the set of equations:

$$J = u(C_i^{\gamma'\gamma} - C_i^{\gamma\gamma'}) \qquad i = 1...n \tag{3.9}$$

where J is the diffusion flux, u is the velocity of the interface and $C_i^{\gamma'\gamma}$, and $C_i^{\gamma\gamma'}$ are the concentrations of the element i in γ in equilibrium with γ', and in γ' in equilibrium with γ respectively. According to Fujita and Bhadeshia [6], when two solids have significantly different diffusivities, the tie-line which

allows the set of set of equations 3.9 to be simultaneously satisfied is the flux-balanced tie-line. As illustrated in Figure 3.2 for a ternary system, flux-balance tie-line passing through M is in general different form the mass-balanced tie-line passing through P.

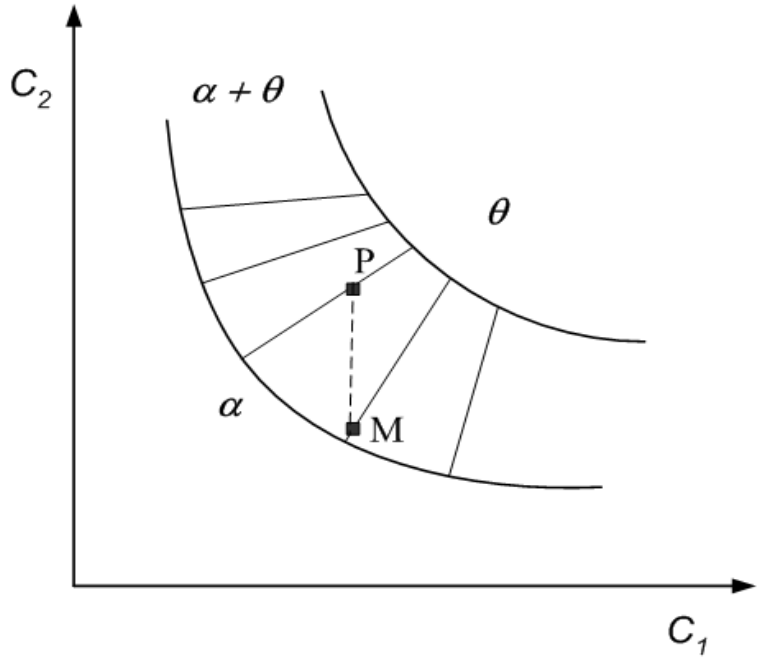

Figure 3.2: The flux-balance tie-line going through M and the mass-balance tie-line passes through P (the bulk composition) for a ternary alloy [6].

In the case where the velocity of the interface is less than an order of magnitude different for the two elements, the flux-balance tie-line is similar to the mass-balanced tie-line that

is passing through $\overline{c_i}$, where i in this case is Al and Ti. In the last case, a treatment of the γ-γ' growth as a binary system is a good first approximation.

Karunaratne *et al.* attempted to obtain estimates of the four ternary interdiffusion coefficients in γ [7]. As expected, both the minor coefficients $D^{\mathrm{Ni},\gamma}_{\mathrm{Al,Ti}}$ and $D^{\mathrm{Ni},\gamma}_{\mathrm{Ti,Al}}$ were almost an order of magnitude smaller than the major coefficients $D^{\mathrm{Ni}\gamma}_{\mathrm{Al,Al}}$ and $D^{\mathrm{Ni},\gamma}_{\mathrm{Ti,Ti}}$. This observation indicates that the diffusion fluxes of Al and Ti are mainly governed by their own concentration gradients

and the influence of the gradients of the other elements is relatively small. Hoshino *et al.* revealed a deviation of the linear plot of the major diffusion coefficients at temperatures below 1373 K [25]. However, according to observations by Karunarante *et al.* the plot of both, major and minor coefficients obeyed the linear relationship of Arrhenius equation [7] provided below:

$$D = D_0 \exp\left(\frac{-Q^*}{RT}\right) \tag{3.10}$$

where Q^* and D_0 are the activation energy and the frequency factor respectively. As expected, the diffusion coefficients show a high sensitivity to temperature. The program calculates the diffusion coefficient at each time step taking into account the current temperature.

The data for the inter-diffusion of Al and Ti indicate that their activation energies and the frequency factors of Al and Ti are very similar resulting in a similar value for their diffusion coefficient at a particular temperature [7].

The program was executed several times, each time configured to use one of two diffusion control components, Al or Ti. Based on the results, the velocity of the interface was almost the same for the Al diffusion control and the Ti diffusion control:

$$v(C_{\mathrm{Ti}}^{\gamma'\gamma} - C_{\mathrm{Ti}}^{\gamma\gamma'}) = -D_{\mathrm{Ti}} \frac{\theta c_{\mathrm{Ti}}}{\theta z}\bigg|_{r=r^*} \tag{3.11}$$

$$v(C_{\mathrm{Al}}^{\gamma'\gamma} - C_{\mathrm{Al}}^{\gamma\gamma'}) = -D_{\mathrm{Al}} \frac{\theta c_{\mathrm{Al}}}{\theta z}\bigg|_{r=r^*} \tag{3.12}$$

where r^* is the position of the interface. The second part of the equations give the diffusion flux towards the interface. According to the calculations, the first part of the equations is less than an order of magnitude different; hence the diffusion flux towards the interface is almost the same in both cases.

According to the model calculations and Karunaratne *et al.* observations, the similarity of the diffusion fluxes validates the assumption of a pseudobi-

nary system, where Al controls the growth rate; hence there is no need to use the tie-line approximation proposed by Fujita and Bhadeshia. Consquently, the program only calculates the activation energy and the frequency factor of Al that corresponds to the initial Al composition of the alloy.

For the values of activation energy of Al, Q^*_{Al}, and of the frequency factor, $D_{0,\mathrm{Al}}$, corresponding to different Al concentrations (obtained by experiments performed by Karunarante *et al.*) it was found that the following second and third order polynomial equations made the best fit with correlation coefficients for $R = 0.98$. These equations are given in Table 3, and their range of applicability for the values of Al concentration is between 1 wt% Al and 7 wt% Al [7].

Q^*_{Al} (kJ/mole)	$y = (-342.59 * c^3_{\mathrm{Al}}) + (2972.2 * c^2_{\mathrm{Al}}) - (2685.2 * c_{\mathrm{Al}}) + 263333$
$D_{0,\mathrm{Al}}(\mathrm{m}^2/\mathrm{s})$	$y = (0.00003 * c^2_{\mathrm{Al}}) + (0.00009 * c_{\mathrm{Al}}) - 0.00004$

Table 3.1: Polynomial equations that give the values of Q^*_{Al} and $D_{0,\mathrm{Al}}$ corresponding to different Al concentrations, c_{Al}.

3.7 Model Implementation

The γ' precipitation model is implemented using FORTRAN and interfaces with MT-DATA. The most important inputs to the program are the composition of the alloy and the temperature that initiates the ageing. Furthermore, the program acquires information for the lattice parameters and the number of atoms per unit cell to derive the molar volume of each phase. Nucleation site density and interfacial energy are required as inputs to calculate the nucleation rate of γ' precipitates. A file is created in MT-DATA for the specific alloy composition and contains the thermodynamic database of the alloy. This file is a reduced database for the phases of interest and is

used as input to the program. Figure 3.3 shows a flow diagram explaining the logic behind the FORTRAN program that implements the model.

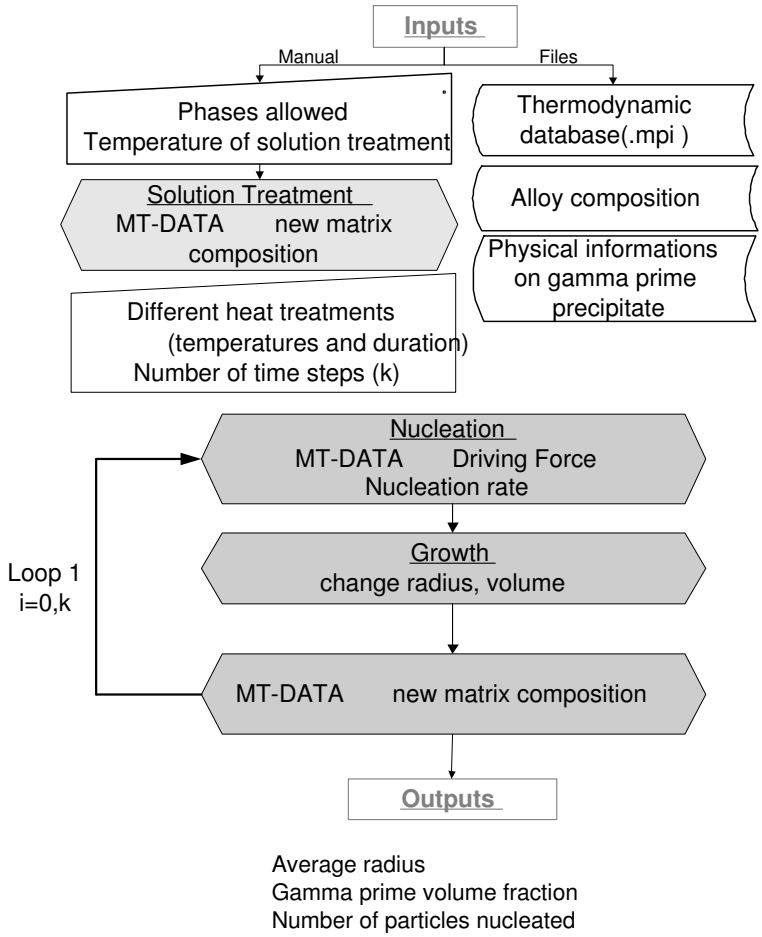

Figure 3.3: Simplified flow-diagram of the FORTRAN propram written to estimate the evolution of the gamma prime precipitation.

The program assumes equilibrium at the solution treatment temperature and calculates a new bulk composition. The Al diffusion coefficient is calculated for the ageing temperature and the program determines the new γ' nuclei that are formed. During a time step the program calculates the growth of the nucleated particles, the change in the volume fraction and by interfacing with MT-DATA updates the matrix composition. As shown in Figure 3.3, Loop 1 is repeated according to the number of steps of the calculation

that are selected as an input to the program. The program displays the average radius, the total number, and the volume fraction of secondary γ' precipitates.

The total time for the calculation is increased in proportion to the number of calculation steps and in proportion to the number of components that the alloy consists of. A typical calculation requires 20000 time steps to calculate the final volume fraction of γ' precipitates in the alloy. Reducing the number of time steps from 20000 to 10000 can lead to a change of the total time from 4 hour to 30 minutes. The number of elements that MT-DATA has sufficient data to deploy depends on the selected database. The databases are constantly upgraded. The maximum number of elements employed in the current calculations is thirteen elements.

3.8 Summary

In this chapter, a FORTRAN program was introduced that deals with the precipitation of secondary γ' particles during ageing in multicomponent systems at different temperature rates . This model applies the classical theory of nucleation and access information from MT-DATA to calculate the driving force of nucleation. For the stage of growth this model employs Zener model and Avrami theory, taking into account the corrections of the extended volume. It was shown that there was no need to implement the flux-balanced tie-line method to deal with multicomponent diffusion, and a binary approximation was used. Al is assumed to control the growth rate and its diffusion coefficient is calculated at different temperatures and for different Al concentrations.

The program transcript is given in Appendix B.

Chapter 4

Simulation Results

The FORTRAN program developed to implement the γ' precipitation model (Section 3.7, Chapter 3) provides a quantitative estimate of the volume fraction of γ' precipitates as a function of composition and heat treatment. It calculates the volume fraction, the average radius, and the total number of secondary γ' precipitates, γ' fine particles that are formed during ageing, at different time intervals. In this chapter, the input parameters of the program are first estimated so that they produce results that match a specified set of the experimental data. The sensitivity of the program in different alloy compositions, temperatures, and cooling rates is then investigated. Plots are used to present the results obtained.

4.1 Fitting Parameters

Equation 3.2 in Chapter 3 has two parameters, nucleation site density, N, and interfacial energy per unit area, σ, that need to be determined. The literature does not provide accurate values for these two parameters. However, physical constraints limit the range of values that can be assigned to σ and N [26]. The program allows for different values of σ and N to be used.

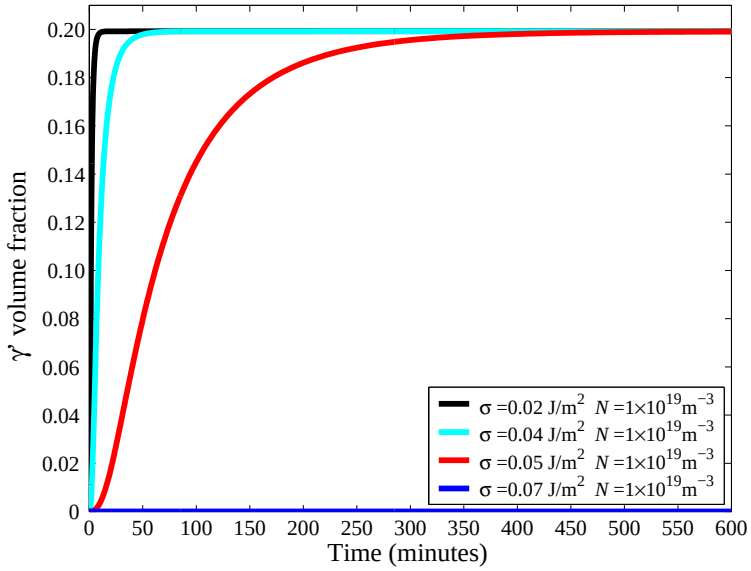

Figure 4.1: Sensitivity of the predicted γ' volume fraction of an Ni-20Cr-2.6Ti-1.58Al alloy to different values of σ, for a fixed value of N=1 $\times$ 10^{19} m^{-3} (solution treatment temperature is 1262 °C, no primary γ'precipitates estimated, ageing temperature is 750 °C for 100 hours, time step 20000).

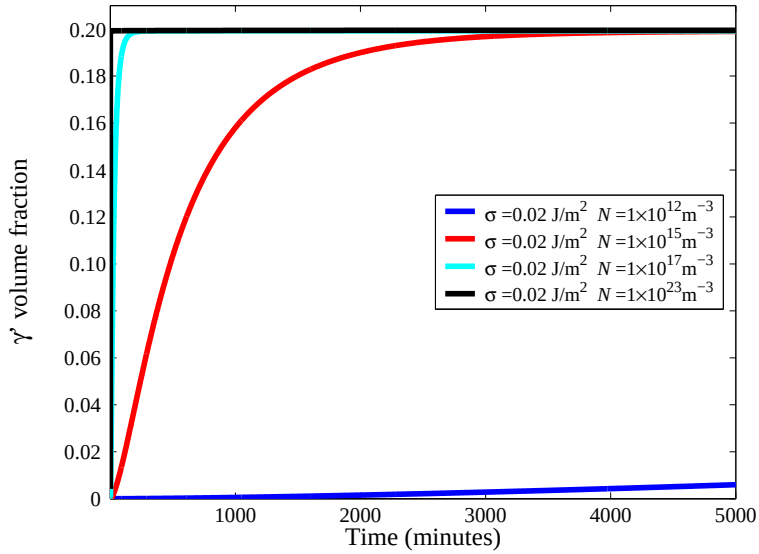

Figure 4.2: Sensitivity of the predicted γ' volume fraction of an Ni-20Cr-2.6Ti-1.58Al alloy to different values of N, for a fixed value of σ=0.04 J/m^2 (solution treatment temperature is 1262 °C, no primary γ'precipitates estimated, ageing temperature is 750 °C for 100 hours, time step 20000).

Figure 4.1 and Figure 4.2 illustrate the sensitivity of the growth rate and the total volume fraction of γ' precipitates for different values of N and σ. σ ranges from 0.02 J/m^2 to 0.07 J/m^2 while keeping N fixed (1×10^{19} m^{-3}), and N ranges from 1×10^{19} m^{-3} to 1×10^{23} m^{-3} while keeping σ fixed (0.04 J/m^2). The influence of these two parameters is significant. In the case of an Ni-20Cr-2.6Ti-1.58Al alloy, even a small change of the interfacial energy from 0.04 J/m^2 to 0.07 J/m^2 can result in almost three orders of magnitude difference in the value of the γ' volume fraction. The average diameter of the γ' particles at the last stage of the precipitate ageing is inversely proportional to N. In the case of an Ni-20Cr-2.6Ti-1.58Al alloy, for a value of σ equal to 0.02 J/m^2 and N in the range between 1×10^{10} m^{-3}and 1×10^{17} m^{-3} result in values of average radius that vary from 5 nm to 2950 nm.

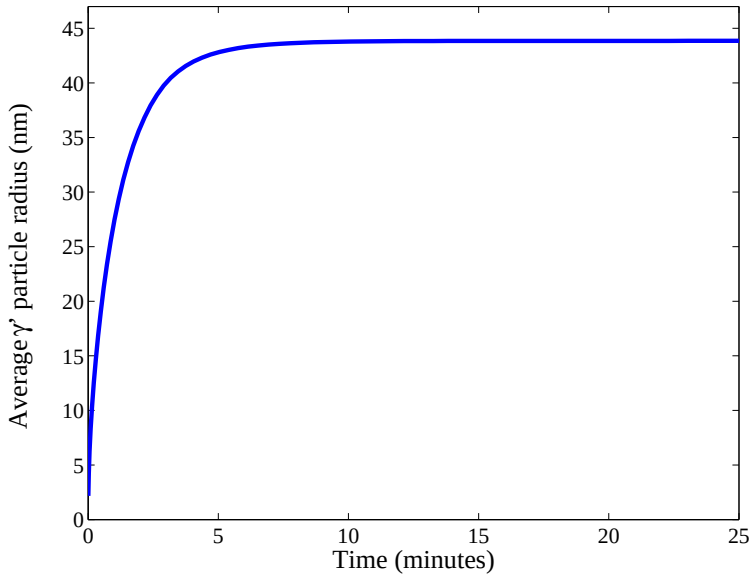

Figure 4.3: Evolution of the calculated average radius of γ' particles during ageing for an Ni-20Cr-2.6Ti-1.58Al alloy and for a value of σ equal to 0.02 J/m^2 and N equal to 1 $\times 10^{19}$ m^{-3} (solution treatment temperature is 1262 °C, ageing temperature is 750 °C for 100 hours, time step 20000).

For N equal to 1×10^{19} m^{-3} and σ equal to 0.02 J/m^2 the average γ' particle radius is 45 nm. The values of the average radius must be an over-

estimate, since the calculations are done in extended space. In the case of Ni-20Cr-2.6Ti-1.58Al alloy the γ' volume fraction of γ' precipitates is less than 0.2. Such a low γ' volume fraction reduces the probability of a large error in the calculated value of the average radius. The calculated average radius γ' particles in an Ni-20Cr-2.6Ti-1.58Al alloy come in agreement with the values obtained from the experimental data [27]. Figure 4.3, shows the average radius of the γ' particles plotted with respect to time. The rate of growth of the particle's average radius decreases with respect to time as expected from the growth theory that predicts that the thickness should be proportional to $t^{1/2}$, during the early stages of ageing until the composition of γ' precipitates is in equilibrium with the matrix and the growth of the precipitates is terminated.

There is no experimental data specifying the time that the precipitation process is finalised. Based on the results, the final radius of the γ' precipitates during growth is obtained at a very early stage (after only a few minutes elapsed). In most cases the precipitation phenomena completed in 1 hour but as the ageing temperature increased and the wt% of Al and Ti was high, the total time to achieve the final volume fraction decreases. In the case of astroloy and IN-100 alloy, where the γ' volume fraction is over 0.5 and the ageing temperature is over 827 ^{o}C, the total time required to obtain the final volume fraction is reduced to 1 minute [23], [24].

Figure 4.4 illustrates that a large value of the interfacial energy hinders γ' precipitate nucleation phenomena, while a large value of N can compensate for this. Decrease of the number of γ' nucleation sites leads to a delay in obtaining the final volume fraction. Formation of nuclei occurs on a very short timescale. In most of the cases investigated it is finalised during the first 2 minutes. Hence, the delay in obtaining the final volume fraction is caused by the stage of the diffusion-controlled growth of the precipitates. For a lower number of nucleation sites more time is required for γ' precipitates

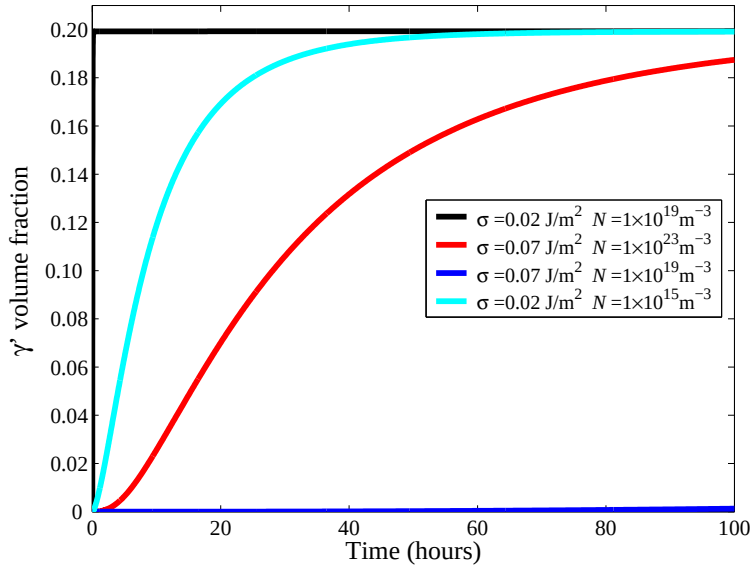

Figure 4.4: Sensitivity of the predicted γ' volume fraction of Ni-20Cr-2.6Ti-1.58Al alloy for different value pairs of N and σ (solution treatment temperature is 1262 °C, no primary γ'precipitates estimated, ageing temperature is 750 °C for 100 hours, time step 20000).

to grow and reach equilibrium.

Measured γ' volume fractions for a number of different alloys with different heat treatments are compared with the ones calculated using the program for different values for N and σ. A choice of high values for the nucleation site density and the interfacial energy underestimates the γ' volume fraction for high temperatures and overestimates it for lower temperatures.

Values of different pairs of σ and N were fitted to adjust the results to the observations of experiments made on a number of different alloys based on nickel with $\sim$ 20% chromium and hardened by different quantities of aluminium and titanium, performed by Gibbons and Hopkins [27]. Taking into account physical constrains on the values assigned to σ and N, the best fit was obtained for N=1 $\times$ 10^{19} m^{-3} and σ=0.01 J/m^2. These values are found to satisfy all compositions over a range of temperatures. We use these values throughout the program calculations that follows. For the chosen values of N and σ, the average γ' particle radius ranges from 45 nm to 150

nm. and the number of γ' precipitates ranges from 1 $\times 10^{-10}$.to 10 $\times 10^{-9}$ at the termination of the growth process. This comes in agreement with the values obtained in the literature [27].

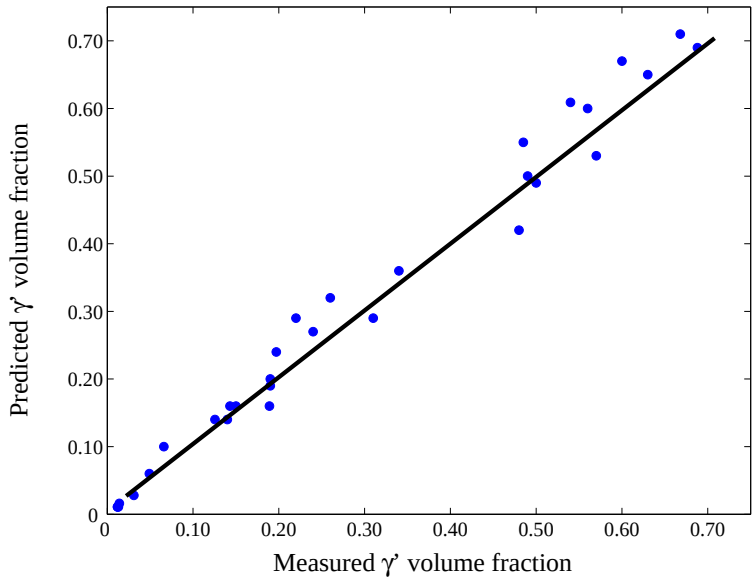

Figure 4.5: Comparison of measured and predicted γ' volume fraction (time step is 20000).

The values of γ' volume fraction that are used to evaluate the model varies between 0.01 and 0.69, the ageing temperature vary between 659 °C and 871 °C [1], [22], [23], [24], [27], [28], [29], [30], [31], [32], [33], [34], [35], [36], [37], [38], [39]. All the experimental data used to evaluate the model are presented in Appendix A. From Figure 4.5 it can be seen that the difference between the predicted and the measured volume fraction is in all cases was less than 0.07 and in most cases it range between 0.02 and 0.04. It is worth noting that a difference between 0.02 to 0.04 in the measured versus predicted volume fraction is within the error margins of the experimental methods used.

4.2 Alloy Composition

Different compositions for alloys based on nickel with 20 wt% chromium and hardened by different quantities of aluminium and titanium are arbitrarily chosen to test the dependence of the γ' volume fraction on certain elements. According to the results obtained, the volume fraction of precipitates is proportional to the total wt% concentration of Al and Ti.

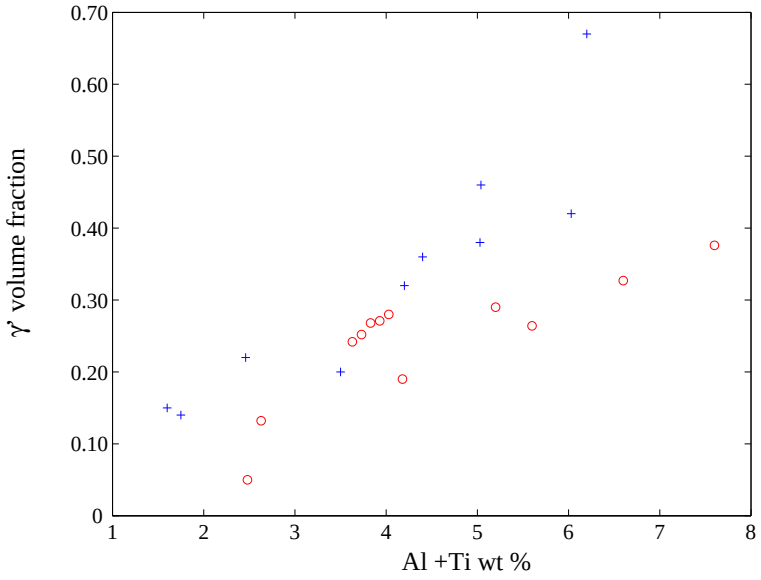

Figure 4.6: Sensitivity of the evolution of γ' precipitates to the total level of Al+Ti wt% for alloys based on nickel with $\sim$ 20% chromium and hardened by different quantities of aluminium and titanium (blue crosses indicate the cases where Al > Ti wt% and red cirlces indicate the cases where Al < Ti wt%) (solution treatment temperature is 1262 °C, no primary γ'precipitates estimated, ageing temperature is 750 °C for 100 hours, time step 20000).

In Figure 4.6 red circles represent the cases where the Ti concentration is chosen to be greater than the Al concentration and blue crosses represent the cases where Al concentration is chosen to be greater than the Ti concentration. The volume fraction of γ' particles has a higher dependence on the wt% Al concentration compared to the wt%Ti concentration. Furthermore, alloys with the lowest Ti to Al ratio are observed to be the ones with the highest

volume fraction. In the case of Al+Ti concentration equal to 6.2 wt%, the predicted volume fraction is 0.69. This can be explained by the fact that the Ti concentration is chosen to be very low, almost 0 wt% [28].

We next consider some of the other elements commonly found in superalloys. In the case of Nb, when added in the Ni-20Cr-2.6Ti-1.58Al alloy and its content in the alloy increases, there is an increase in the growth rate of up to 10%. This is in agreement with published experimental data [23].

Figure 4.7 shows the change of the predicted γ' volume fraction of an Ni-20Cr-2.6Ti-1.58Al alloy caused by a 3 wt% addition of a number of different elements. Alloys containing Ta, W, and Fe, which are slower diffusing, were expected to have a lower growth rate compared to alloys that do not contain these elements (Figure 4.7). However, our calculations indicate an increase in the growth rate of up to 20%. This can be explained by the fact that the model does not take into account the Ta, W, and Fe diffusion but rather, it considers the influence of these elements on the equilibrium matrix composition. Adding Ta, W, and Fe results in a decrease of the equilibrium concentration of Ni, Al, and Ti. Consequently, this leads to an increase of supersaturation. If Ta is substituted with W, this results in a decrease of the final γ' volume fraction by approximately 10% [33].

Zr content has a strong influence on the γ' volume fraction. Adding 3 wt% Zr can lead to a 50% increase in the volume fraction. In contrast, adding 3 wt% C and B can lead to a decrease of more than 50% in the volume fraction (Figure 4.7). Adding C and B results in an increase of the equilibrium concentration of Ni, Al, and Ti. Consequently, this leads to a decrease of supersaturation. Despite these observations, the content of Zr, C, and B in alloys is insufficient to cause any change in the γ' growth rate since it is less than 1 wt%.

If the content of Co and Mo in the alloy is less than 3 wt% this results in a small increase of the γ' volume fraction of up to 10% (Figure 4.7). When

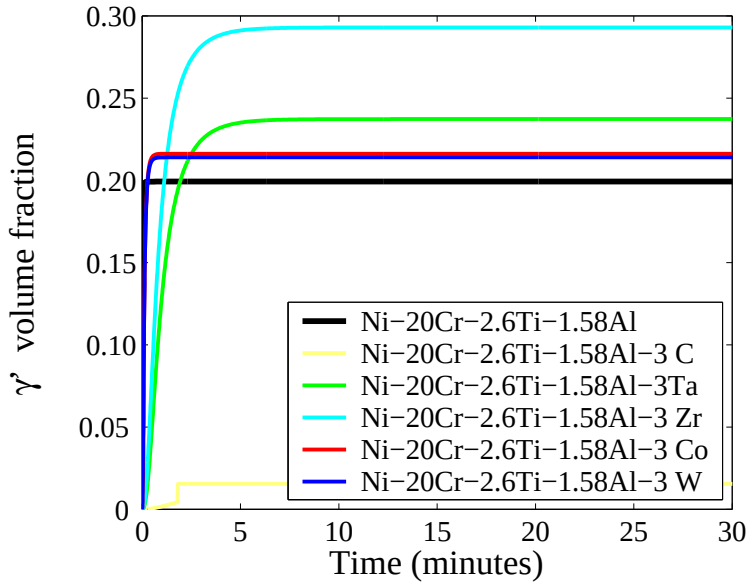

Figure 4.7: Sensitivity of the predicted γ' volume fraction of an Ni-20Cr-2.6Ti-1.58Al alloy to different elements added (solution treatment temperature is 1262 °C, no primary γ'precipitates estimated, ageing temperature is 750 °C for 100 hours, time step 20000).

the content of Co and Mo exceeds 3 wt%, we observe a weak decrease in the volume fraction. This comes in agreement with published experimental data [23].

4.3 Isothermal Ageing

According to the Avrami theory, Section 2.3, Chapter 2, the effect of temperature is to alter the driving force for transformation and the Al diffusion coefficient.

Figure 4.8 illustrates the effects of changing the temperature on the calculated γ' volume fraction. It is obvious that the volume fractions may be changed substantially by the change of temperature during ageing.

For an Ni-20Cr-2.6Ti-1.58Al alloy at temperatures less than 830 °C the precipitation is slow, while at temperatures above 927 °C γ' phase is unstable. The maximum volume fraction is obtained at 730 °C, and is equal to 0.21.

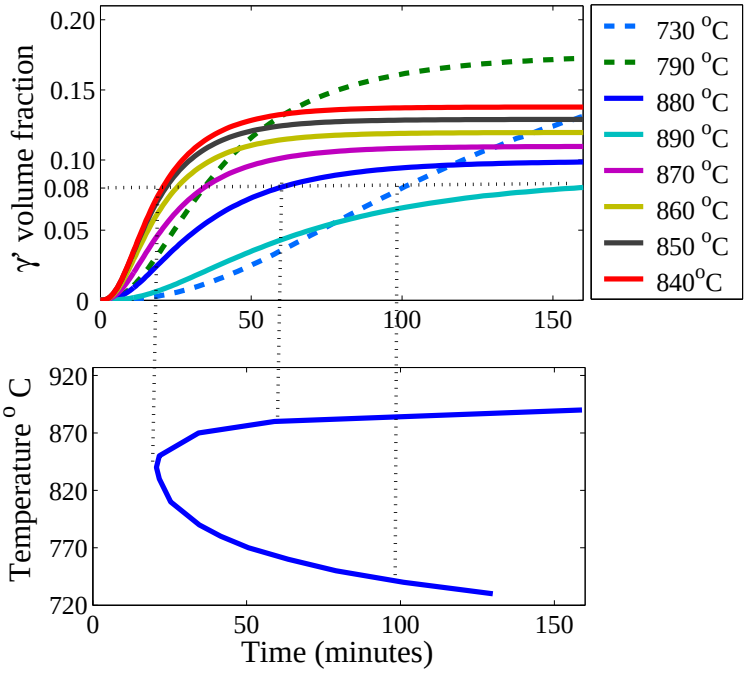

Figure 4.8: Time Temperature Precipitation (TTT) diagram for the formation of predicted γ' phase in an Ni-20Cr-2.6Ti-1.58Al alloy (solution treatment temperature is 1080 °C, no primary γ'precipitates estimated, time step is 20000).

Based on Figure 4.8, a time-temperature-transformation diagram (TTT) can be drawn. The curve corresponds to 0.08 γ' volume fraction. Figure 4.8 correctly shows the growth of the precipitate during prolonged heat treatment at different temperatures. The curve has a typical C shape because the driving force for transformation is small at high temperatures, more than 887 °C, and diffusion is small at low temperatures, less than 827 °C. The optimum temperature for transformation is 840 °C. This combines the driving force for transformation and the diffusion giving a maximum in the rate of reaction.

4.4 Continuous Cooling

The existing program can deal with continuous cooling transformations. The results obtained by the program for a number of different cooling rates

match the published experimental data [34].

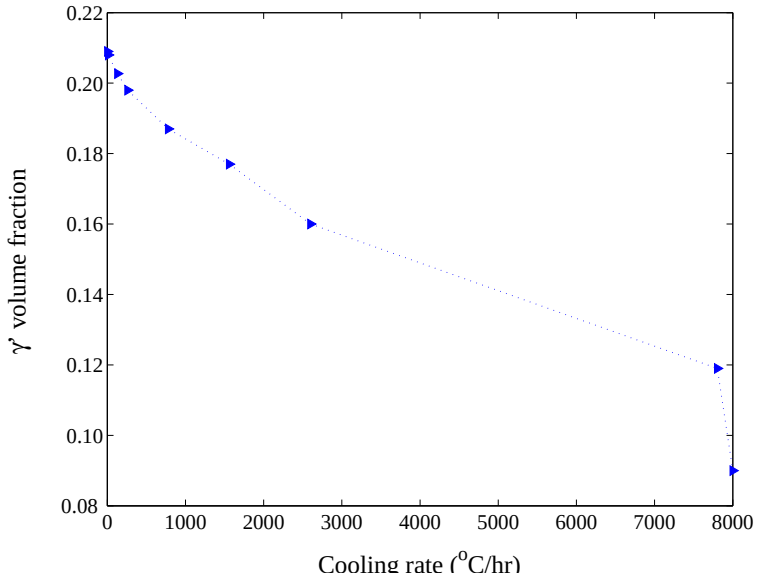

Figure 4.9: γ' volume fraction predicted by the program for an Ni-20Cr-2.6Ti-1.58Al alloy and for different cooling rates (solution treatment temperature is 1080 °C, no primary γ'precipitates estimated, time step is 20000).

Evolution of γ' precipitate volume fraction during continuous cooling is examined by using arbitrary cooling rates as input. According to Figure 4.9, for an Ni-20Cr-2.6Ti-1.58Al alloy a decrease of the cooling rate leads to an increase of the γ' volume fraction. High cooling rates result in uniform particles with small radius (2 nm) since undercooling causes nucleation of additional γ' precipitates. In contrast, decreasing the cooling rate results in larger average radius (20 nm) since there is sufficient time for particles nucleated to grow.

For a decrease in temperature from 860 °C to 730 °C in more than thirty minutes, the volume fraction obtained is almost the same with the volume fraction that results from steady heat treatment at 730 °C. It is worth mentioning that a correct time step needs to be chosen since the program can easily lead to unrealistic results for sudden temperature changes in situations where the matrix composition changes dramatically. Figure 4.10 illus-

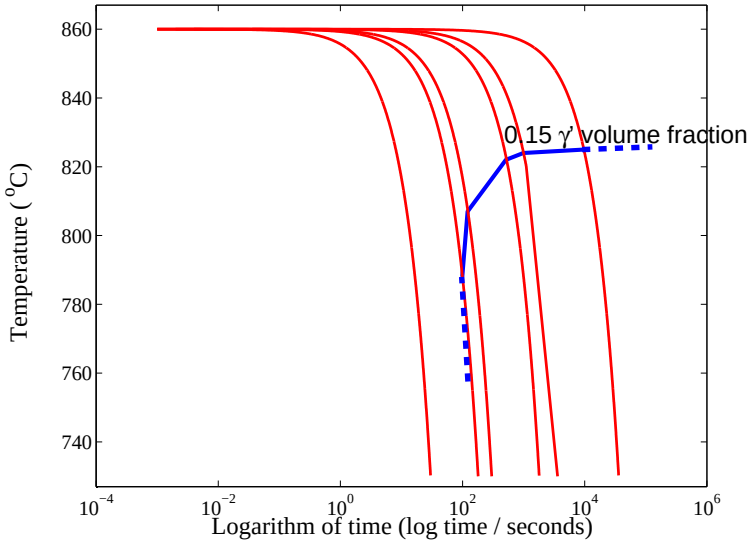

Figure 4.10: Continuous-Cooling-Transformation (CCT) diagram for the formation of predicted γ' phase in an Ni-20Cr-2.6Ti-1.58Al alloy (solution treatment temperature is 1080 °C, time step is 20000).

trates the 0.15 γ' volume fraction for different cooling rates. The Continuous-Cooling-Transformation diagram comes in agreement with typical TTT diagrams. This indicates that the model produces reasonable results for different cooling rates.

4.5 Summary

In this chapter, the values of interfacial energy, σ, and number of nucleation sites, N, were fitted to adjust the results to the observations of experiments performed by Gibbons and Hopkins. The best fit was obtained for the values of N equal to 1×10^{19} m^{-3} and σ equal to 0.01 J/m^2. These values were used throughout the program calculations that followed. The program was evaluated using data obtained in the literature. The values of the γ' volume fraction that were used to evaluate the model varied between 0.01 and 0.69. The model results came in agreement with the measured data and are within a 10 % error margin. The average radius of γ' precipitates

ranged from 45 nm to 150 nm, and the number of γ' precipitates ranged from 1 $\times 10^{-10}$ to 10 $\times 10^{-9}$.

Next, the sensitivity of our model to different alloy compositions was investigated. Using alloys based on nickel with 20 wt% chromium hardened by different quantities of aluminium and titanium it has been shown that the γ' volume fraction is proportional to the total Al + Ti wt% content and more specific of the Al:Ti content ratio. When Nb is added to the alloy there is a small increase in the volume fraction of up to 2%. All the other elements considered do not cause a significant change to the γ' volume fraction due to their low concentration (less than 1 wt%). Nevertheless, adding 3 wt% Ta, W, Fe, and Zr leads to an increase of the γ' volume fraction of up to 50%. In contrast, adding 3 wt% C and B leads to a 50% decrease of the γ' volume fraction.

The effect of temperature on the γ' volume fraction was also investigated. An increase of the temperature up to values lower than the γ' solvus temperature leads to a decrease of the total γ' volume fraction. A typical C shape Time-Temperature-Transformation (TTT) was produced after plotting the results for an Ni-20Cr-2.6Ti-1.58Al alloy and for 0.08 volume fraction. Finally, arbitrary cooling rates were used as input to the model. It has been shown that a decrease in the cooling rate leads to an increase of the γ' volume fraction, resulting in a typical Continuous-Cooling-Temperature (CCT) diagram.

The results produced by the model for different temperatures, compositions, and cooling rates were found to be reasonably accurate. The model can predict γ' volume fraction of a superalloy within a 10% error margin.

Chapter 5

Conclusions

Nickel-based superalloys are successfully used as components of aircraft engines and power plants, both marine and land based. They present a high creep resistance and stability at high temperatures. The strength of nickel-based superalloys is derived from the presence of γ' precipitates. The main aim of this research was to develop a physical model that would give a quantitative estimation of the volume fraction of γ' precipitates as a function of composition and heat treatment.

A review has been made on previous attempts to model the γ' precipitation process. The problem of predicting the γ' microstructural evolution has been approached by a number of different solutions that were either based on nucleation and diffusion-controlled growth theories or used the phase field method. All the proposed methods failed to predict the nucleation and growth of the fine secondary γ' precipitates in ternary systems during alloy ageing.

A FORTRAN model which interfaces with MT-DATA, a thermodynamic software package, has been created and is capable of predicting the evolution of secondary γ' precipitates in multicomponent and multiphase systems, during ageing. Accurate thermodynamic calculations can be performed using MT-DATA for the phase of nucleation, withought making unnecessary

approximations for the driving force of nucleation and the concentration profile of all the elements. The basic theory of nucleation and growth was employed. Al was assumed to be the controlling component for diffusion-controlled growth and its diffusion coefficient was calculated as a function of temperature and alloy composition.

Values of nucleation site density, N, equal to 1×10^{19} m^{-3}, and interfacial energy per unit area, σ, equal to 0.01 J/m^2 were determined since they result in the best fit with the experimental data. The model was evaluated using data obtained in the literature. The results obtained by the model came in agreement within a 10 % error margin. The sensitivity of this model in different alloy compositions and different temperatures and cooling rates was tested and a number of important results were obtained.

Future research can be conducted to improve the prediction of γ' volume fraction by allowing the model to take into account the primary γ' precipitates that are formed at high temperatures during quenching. It would be useful to extend this model to predict the coarsening of γ' particles. During coarsening, volume fraction remains constant and larger particles grow in expense of smaller ones. Incorporating coarsening in the model will give a more accurate prediction of the alloy microstructure. It is also worth taking into account the capillarity effects during the stage of growth and coarsening, further improving the predictions of the average radius of γ' particles.

Appendix A

Experimental Data

All compositions are given in wt%

Solution treatment : 1080 °C

Ageing Temperature: 700 °C for 16 h [27]

Ni	Cr	Al	Ti	Nb	γ' volume fraction
balance	20.00	3.50	-	-	0.19
balance	20.00	4.20	-	-	0.26
balance	20.00	4.40	-	-	0.34
balance	20.00	6.20	-	-	0.60
balance	20.00	0.85	1.63	-	0.05
balance	20.00	1.58	2.60	-	0.19
balance	20.00	2.20	3.00	-	0.31
balance	20.00	1.75	-	4.90	0.15
balance	20.00	1.60	-	6.30	0.15
balance	20.00	2.40	-	6.30	0.22

Solution treatment : 1200 °C

Ageing Temperature 870 °C for 24 h [28]

Ni	Cr	Al	Ti	Fe	C	Co	Mo	γ'volume fraction
balance	15.00	3.00	2.20	0.70	0.12	28.5	3.70	0.19

Solution treatment : 1150 °C

Ageing Temperature 850 °C for 16 h - 800 °C for 100 h [29]

Ni	Cr	Al	Ti	Co	Mo	Nb	γ' volume fraction
balance	24.20	1.49	2.93	19.30	1.44	1.44	0.24
balance	24.15	1.34	2.66	19.90	1.53	0.93	0.19
balance	24.15	0.84	1.48	19.80	1.52	0.58	0.66
balance	24.1	0.70	1.29	19.8	1.55	0.48	3.1

Solution treatment : 1080 °C

Ageing Temperature 850 °C for 4 h - 760 °C for 16 h [22]

Ni	Cr	Al	Ti	Co	Mo	γ' volume fraction
balance	19.50	1.30	3.00	13.50	4.30	0.89

Solution treatment : 1302 °C

Ageing Temperature 871 °C for 20 h [23]

Ni	Cr	W	Al	Ti	C	Co	Mo	B	Ta	γ' volume fraction
balance	9.20	9.20	5.20	1.40	-	-	0.70	-	-	0.49
balance	9.20	10.20	5.70	1.40	0.01	-	1.00	-	2.82	0.57
balance	8.60	11.80	5.30	1.40	0.01	-	0.60	0.01		0.54
balance	8.80	9.00	5.20	1.40	-	5.20	0.70	-		0.49
balance	8.50	9.90	5.20	1.40	-	5.00	0.60	-	2.98	0.56
balance	8.90	9.00	5.30	1.40	-	10.10	-	-	-	0.48
balance	8.50	9.70	5.20	1.40	0.01	10.10	-		2.80	0.55
balance	8.60	11.70	5.30	1.20	-	10.10	3.00			0.53

Solution treatment : 1310 °C

Ageing Temperature 850 °C for 24h [24]

Ni	Cr	W	Al	C	Co	Ta	γ' volume fraction
balance	8.00	8.00	6.10	-	2.00	6.00	0.67
balance	8.00	8.00	6.10	5.00	2.00	6.00	0.68
balance	8.00	8.00	6.10	7.50	2.00	6.00	0.69

Solution treatment : 1117 °C

Ageing Temperature 650 °C for 24 h [35]

Ni	Cr	Al	Ti	Fe	C	Co	Mo	B	Ta	Zr	γ' volume fraction
balance	14.00	3.31	2.41	0.18	0.08	7.71	3.33	0.01	3.42	0.06	0.52

Solution treatment : 1117 °C

Ageing Temperature 982 °C for 4 h [35]

Ni	Cr	Al	Ti	Fe	C	Co	Mo	B	Zr	γ' volume fraction
balance	12.20	4.71	4.19	0.08	0.34	17.80	3.20	0.02	0.05	0.58

Solution treatment : 1117 °C

Ageing Temperature 650 °C for 24 h [35]

Ni	Cr	Al	Ti	Fe	C	Co	Mo	B	Zr	γ' volume fraction
balance	12.20	4.88	4.17	0.08	0.08	18.30	3.39	0.02	0.04	0.63

Solution treatment : 1080 °C

Ageing Temperature 750 °C for 16h [36]

Ni	Cr	Al	Ti	C	Nb	B	γ' volume fraction
balance	20.00	0.95	2.90	0.04	-	0.01	0.13
balance	20.00	0.95	2.90	0.04	0.51	0.01	0.13
balance	20.00	0.95	2.90	0.04	1.0	0.01	0.14
balance	20.00	0.95	2.90	0.04	1.24	0.01	0.15
balance	20.00	0.95	2.90	0.04	1.53	0.01	0.15
balance	20.00	0.95	2.90	0.04	1.72	0.01	0.15
balance	20.00	0.95	2.90	0.04	1.94	0.01	0.16
balance	20.00	0.95	2.90	0.04	2.46	0.01	0.16

Solution treatment : 1145 °C

Ageing Temperature 982 °C for 75 minutes - 732 °C for 8 h [34]

Ni	Cr	Al	Ti	Mo	V	C	γ' volume fraction
balance	12.40	5.00	3.00	3.20	12.40	0.07	0.29

Appendix B

FORTRAN Program

MAP_NICKEL_GAMMA_PRIME

This appendix presents the model described in Chapter 3 and associated documentation following the MAP format,
http://www.msm.cam.ac.uk/map/mapmain.html.

1 Provenance of Source Code

Plati Aikaterini and Sourmail T.
Phase Transformations and Complex Properties Group,
Department of Materials Science and Metallurgy,
University of Cambridge,
Cambridge, CB2 3QZ,
United Kingdom.

This program is interfaced with MT-DATA:
National Physical Laboratory,
Teddington,
Middlesex, TW11 0LW,
United Kingdom.

Added to MAP: August 2003.

2 Purpose

A program for the prediction of secondary γ' volume fraction during ageing, as a function of alloy composition, cooling rate, temperature and time.

3 Specification

Language: FORTRAN

Product Form: Source Code

Operating System: tested on Linux.

4 Description

MAP_NICKEL_GAMMA_PRIME contains the program which enables the user to predict the volume fraction of secondary γ' precipitates as a function of chemical composition, temperature, cooling rate and time. All thermodynamic calculations are performed internally by MT-DATA. The software uses MTDATA.mpi database file which has to be created earlier by the user, using the ACCESS module of MT-DATA. Once uncompressed, MAP_NICKEL_GAMMA_PRIME contains:

gamma_prime.f

The source code for the program.

compile

A unix shell script to compile the program and link it to MT-DATA object files.

precipitate_data

A file which contains information about γ' precipitates, that is, lattice parameter, number of atoms per unit cell, and parameters of nucleation (nucleation site density and intefacial energy).

spheregrowth.out, planargrowth.out

Contains 500 precalculated points for the solution to the sphere growth and planargrowth equations as described in [1].

README

A text file containing instructions for running the program.

5 References

1. Plati Aikaterini, Master of philosophy (M.Phil) thesis, Chapter 3, University of Cambridge, 2003.

6 Input Parameters

The user is required to provide the alloy chemical composition, the solution temperature, the number of heat treatments, the maximum and minimum temperature and the duration of every heat treatment.

7 Output Parameters

The default outputs are:

The time (seconds) - the average radius (m) - the secondary γ' volume fraction - the total number of secondary γ' precipitates - the temperature (K).

Keywords

secondary gamma prime, precipitation, volume fraction, gamma prime, ageing.

Example

I. Program Test

Complete program

II. Program Data

File named test.mpi. The composition of the superalloy is Ni 75.82 wt%,

Cr 20 wt%, Ti 2.6 wt% and Al 1.58 wt% and is included in a file named try-composition. The number of timesteps is 2000. The solution treatment is 1353 K and the ageing temperature 1023 °C for 100 h. The input.dat file is as follows:

0.5, 1.58, 1, test, n, n, 2, 1, 0, 1, 2, 0, 1353, n, n, 1, 3, 1, 1023, 1023, 360000, 20000, 360000, output

III. Program Results

In the file output we obtain the following results:

.900000E-01 .108542E-08 .130426E-07 .230067E+17 .102300E+04

.360000E+00 .210832E-08 .359687E-06 .924163E+17 .102300E+04

.810000E+00 .311700E-08 .257766E-05 .207052E+18 .102300E+04

.144000E+01 .412265E-08 .105008E-04 .365351E+18 .102300E+04

.225000E+01 .512966E-08 .312733E-04 .565157E+18 .102300E+04

.324000E+01 .614066E-08 .762638E-04 .803766E+18 .102300E+04

.441000E+01 .715752E-08 .161845E-03 .107797E+19 .102300E+04

.576000E+01 .818170E-08 .309994E-03 .138413E+19 .102300E+04

.729000E+01 .921433E-08 .548670E-03 .171822E+19 .102300E+04

.900000E+01 .102562E-07 .911904E-03 .207589E+19 .102300E+04

.108900E+02 .113079E-07 .143954E-02 .245259E+19 .102300E+04

.129600E+02 .123695E-07 .217656E-02 .284361E+19 .102300E+04

.152100E+02 .134407E-07 .317192E-02 .324417E+19 .102300E+04

.176400E+02 .145208E-07 .447695E-02 .364954E+19 .102300E+04

.202500E+02 .156086E-07 .614313E-02 .405511E+19 .102300E+04

.230400E+02 .167026E-07 .821955E-02 .445651E+19 .102300E+04

.260100E+02 .178006E-07 .107500E-01 .484967E+19 .102300E+04

.291600E+02 .189000E-07 .137700E-01 .523093E+19 .102300E+04

.324900E+02 .199980E-07 .173040E-01 .559708E+19 .102300E+04

.360000E+02 .210911E-07 .213630E-01 .594542E+19 .102300E+04

.396900E+02 .221760E-07 .259427E-01 .627382E+19 .102300E+04

.435600E+02 .232489E-07 .310234E-01 .658069E+19 .102300E+04

.476100E+02 .243063E-07 .365700E-01 .686496E+19 .102300E+04

.518400E+02 .253446E-07 .425334E-01 .712609E+19 .102300E+04

.....

.358561E+06 .439900E-07 .199316E+00 .878188E+19 .102300E+04

.358921E+06 .439900E-07 .199316E+00 .878188E+19 .102300E+04

.359280E+06 .439900E-07 .199316E+00 .878188E+19 .102300E+04

.359640E+06 .439900E-07 .199316E+00 .878188E+19 .102300E+04

.360000E+06 .439900E-07 .199316E+00 .878188E+19 .102300E+04

Bibliography

[1] Baldan A. *Z. Metallkd*, 83:324–330, 1992.

[2] Sourmail T. *Simultaneous Precipitation Reactions in Creep–Resistant Austenitic Stainless Steels*. PhD thesis, University of Cambridge, 2002.

[3] McLean D. *Metal Science*, 18:249–256, 1984.

[4] Gabb T., Backman D., Ewi D. Y., Mourer D., Furrer D., Garg A., and Ellis D. pages 405–414, 2000.

[5] Wang Y. and Khachaturyan A. G. *Acta Mater*, 31:2983–3000, 1994.

[6] Bhadeshia H. K. D. H. *Progress in Materials Sci.*, 29:322–383, 1985.

[7] Karunarante M. S., Carter P., and Reed R. C. *Acta mater*, 49:861–875, 2001.

[8] Christian J. W. *Theory of Transformations in Metals and Alloys*. Pergamon Press, Oxford, 1965.

[9] Grosdidier T., Hazotte A., and Simon A. *Materials Science and Engineering*, A256:183–196, 1998.

[10] Cahn R. W., Haasen P., and Kramer E. J. *Materials Science and Technology*, volume 8. VCH, 1996.

[11] Smallman R. E. and Bishop R. J. *Metals and Materials*. Butterworth and Heinemann, 1995.

[12] Trancet F., Sourmail T., Yescas M. A., Evans R. W., McAleese C., Singh L., Smeeton T., and Bhadeshia H. K. D. H. *Material Science and Technology*, 19:296–303, 2003.

[13] Van der Ven A. and Delaey L. *Progress in Materials Science*, volume 40. ELSEVIER Sience Ltd, 1996.

[14] Gessinger G. H. *Powder Metallurgy of Superalloys*. BMM, 1984.

[15] Coates D. E. *Metall. Trans.*, 3:1203–1212, 1972.

[16] Coates D. E. *Metall. Trans.*, 4:1077–1086, 1973.

[17] Fujita N. and Bhadeshia H. K. D. H. *Mater. Sci. Techn.*, 15:627–634, 1999.

[18] Irisarri A. M., Urcola J. J., and Fuentes M. *Material Science and Technology*, 1:516–519, July 1985.

[19] Simmons J. P., Shen C., and Wang Y. *Scripta mater*, pages 935–342, 2000.

[20] MTDATA. National Physical Laboratory, Teddington, Middlesex, U.K., 1989.

[21] National Physical Laboratory (NPL). Mtdata, http://www.npl.co.uk/npl/cmmt/mtdata/, 2003.

[22] Wosik J., Dubiel B., Kruk A., Penkalla H. J., Schubert F., and Czyrska-Filemonowicz A. *Materials Characterization*, 46:119–123, 2001.

[23] Nathal M. V. and Ebert L. J. *Superalloys 1984*, pages 125–133, 1984.

[24] Khan T., Caron P., and Duret C. *Superalloys 1984*, pages 145–155, 1984.

[25] Hoshino K., Rothman S. J., and Averback R. S. *Acta metall*, 36:1271–1277, 1988.

[26] Saunders N. and Miodownik A. P. *Metallurgical and Materials Transactions*, 33A:2002–3367, 2002.

[27] Gibbons T. B. and Hopkins B. E. *Metal Science Journal*, 5:233–240, 1971.

[28] Koul A. K. and Wallace W. *Metallurgical Transactions A*, 13A:673–675, 1982.

[29] Gibbons T. B. and Hopkins B. E. *Metal Science*, 18:273–280, 1984.

[30] Roebuck B., Cox D., and Reed R. *Scripta Mater*, 44:917–921, 2001.

[31] Royer A., Bastie P., and Veron M. *Acta Mater*, 15:5357–5368, 1998.

[32] Ducki K. J., Hetmanczyk M., and Kuc D. *Materials Chemistry and Physics*, 9816:1–3, 2003.

[33] Brinegar J. R., Mihalisin J. R., and VanderSluis J. *Superalloys 1984*, pages 53–60, 1984.

[34] Agnieszka M. Wusatowska-Sarnek, Martin J. Blackburn, and Mark Aindow. *Materials Science Forum*, pages 767–772, 2003.

[35] Kenneth R. Bain and Regis M. Pelloux. *Superalloys 1984*, pages 387–396, 1984.

[36] Encai Guo, Zhiyan Han, and Shuyou Yu. *Superalloys 1984*, pages 583–590, 1984.

[37] Raymond C. Benn. *Superalloys 1980*, pages 541–550, 1980.

[38] Guo E. C. and Ma F. J. *Superalloys 1980*, pages 431–438, 1980.

[39] Chang J. F., Hi G. P., and Gao L. *Superalloys 1980*, pages 245–255, 1980.